Interactive Domains for Chaperone Activity in the Small Heat Shock Protein, Human αB Crystallin†

Joy G. Ghosh,‡,§ Marcus R. Estrada,§ and John I. Clark*,‡,§,||

Biomolecular Structure and Design, Department of Biological Structure, and Department of Ophthalmology, University of Washington, Seattle, Washington 98195-7420

Received March 1, 2005; Revised Manuscript Received June 9, 2005

ABSTRACT: Protein pin arrays identified seven interactive sequences for chaperone activity in human αB crystallin using natural lens proteins, β_H crystallin and γD crystallin, and in vitro chaperone target proteins, alcohol dehydrogenase and citrate synthase. The N-terminal domain contained two interactive sequences, $_{9}$WIRRPFFPFHSP$_{20}$ and $_{43}$SLSPFYLRPPSFLRAP$_{58}$. The α crystallin core domain contained four interactive sequences, $_{75}$FSVNLDVK$_{82}$ (β3), $_{113}$FISREFHR$_{120}$, $_{131}$LTITSSLS$_{138}$ (β8), and $_{141}$GVLTVNGP$_{148}$ (β9). The C-terminal domain contained one interactive sequence, $_{157}$RTIPITRE$_{164}$, that included the highly conserved I-X-I/V motif. Two interactive sequences, $_{73}$DRFSVNLDVKHFS$_{85}$ and $_{131}$LTITSSLSDGV$_{141}$, belonging to the α crystallin core domain were synthesized as peptides and assayed for chaperone activity in vitro. Both synthesized peptides inhibited the thermal aggregation of β_H crystallin, alcohol dehydrogenase, and citrate synthase in vitro. Five of the seven chaperone sequences identified by the pin arrays overlapped with sequences identified previously as sequences for subunit−subunit interactions in human αB crystallin. The results suggested that interactive sequences in human αB crystallin have dual roles in subunit−subunit assembly and chaperone activity.

Human αB crystallin is a small heat shock protein (sHSP) and molecular chaperone. sHSPs are characterized by molecular masses of <43 kDa, a low degree of sequence similarity, upregulation in response to environmental stress, and an ability to protect against the unfolding and aggregation of proteins through activity as molecular chaperones (*1*−*7*). sHSPs are ubiquitous in cells and tissues throughout the plant and animal kingdoms and are upregulated in age-related myopathies, cardiac ischemia, and a variety of protein aggregation diseases, including Alexander's disease, Alzheimer's disease, Creutzfeld-Jakob disease, and Parkinson's disease (*8*−*18*). In the lens where α crystallins comprise approximately 33% of the total protein content, the accumulation of post-translational modifications is associated with protein unfolding that favors attractive interactions between proteins and formation of aggregates that are large enough to result in light scattering and cataract (*19*−*30*). In theory, high concentrations of α crystallins in lens cytoplasm can bind unfolding β/γ crystallin proteins, stabilize transparent cell structure, and protect against aggregation and opacification through their function as molecular chaperones (*31*−*36*). In a normal lens, αB crystallin is a structural protein that interacts weakly with the β/γ crystallins and is closely associated with the filament network (*37*, *38*).

While X-ray crystal structures exist for β and γ crystallin, the structure of αB crystallin is based on spectroscopic data and homology models (*39*−*47*). Spectroscopic data, secondary structure prediction, and X-ray crystal structures of two homologous sHSPs, *Methanococcus jannaschi* (Mj) sHSP16.5 and wheat sHSP16.9, indicated that sHSPs are characterized by three structural domains, an N-terminal domain that varies in primary sequence, an α crystallin core domain that is conserved in terms of primary sequence and secondary structure, and a C-terminal extension that is variable in sequence. In the crystal structures of Mj sHSP16.5 and wheat sHSP16.9, the N-terminal domain is largely helical or unstructured, the α crystallin core domain is an immunoglobulin-like fold, and the C-terminal extension domain protrudes from the α crystallin core domain and is unstructured and flexible (*46*). The immunoglobulin-like fold adopted by the α crystallin core domain is a β sandwich composed of two antiparallel β sheets formed by six to nine β strands connected by loops of variable lengths. The formation of dimers in wheat sHSP16.9 is due to interactions between the β2 and β3 strands of one monomer with the β6 strand contained in the loop connecting β5 and β7 of another monomer. The C-terminal extension contains a conserved I-X-I/V motif, where I is isoleucine, V is valine, and X is any natural amino acid. In wheat sHSP16.9, the I-X-I motif of one monomer interacts with residues of the β4 and β8 strands of another monomer to form the higher-order dodecameric quaternary structure observed in the crystal structure. While αB crystallin contains the same three structural domains found in Mj sHSP16.5 and wheat sHSP16.9, the complex assembly of human αB crystallin is larger and more polydisperse than the two sHSPs that have been crystallized. This suggests that the dimer interface and the oligomerization interface in αB crystallin may be different from those of the smaller homologous sHSPs.

† Supported by Grant EY04542 from the NEI.

* To whom correspondence should be addressed: Department of Biological Structure, HSB G514, Box 357420, University of Washington, Seattle, WA 98195-7420. E-mail: clarkji@u.washington.edu. Phone: (206) 685-0950. Fax: (206) 543-1524.

‡ Biomolecular Structure and Design.

§ Department of Biological Structure.

|| Department of Ophthalmology.

10.1021/bi0503910 CCC: $30.25
Published on Web 10/07/2005

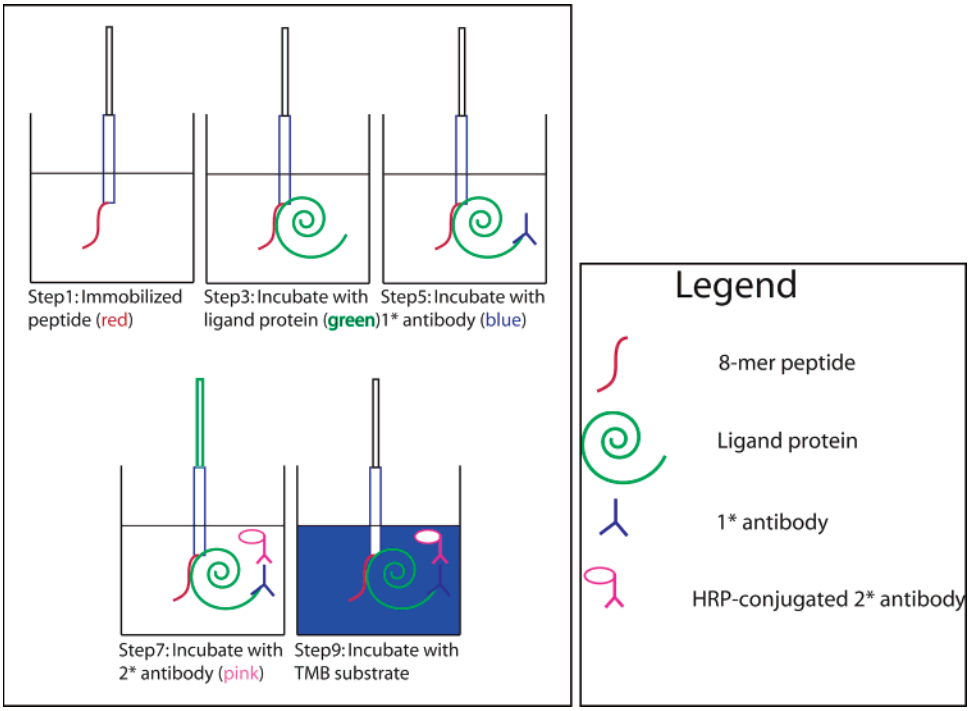

FIGURE 1: Schematic for the protein pin array assay. Refer to Materials and Methods for detailed protocols. The absorbance corresponding to the blue coloration in each well was measured at 450 nm (λ) and plotted against the amino acid sequence of the corresponding peptide in that well (Figures 2 and 3). Wells containing peptides that have strong interactions with target proteins are dark blue, and wells containing peptides that have weak or no interaction with target proteins are light blue or clear.

Proteolysis and domain-swapped chimeric mutants of αB crystallin and *Caenorhabditis elegans* sHSP12.2 indicated that sequences in all three structural domains of sHSPs were important for complex assembly and chaperone activity (*48*, *49*). The identity of specific residues or sequences in each domain important for the complex assembly and chaperone activity of αB crystallin and other small heat shock proteins remains to be determined.

In a previous study using a protein pin array of sequential and overlapping 8-mer peptides of human αB crystallin, the interactive domains required for subunit−subunit interactions and complex assembly in human αB crystallin were identified (*47*). The N-terminal sequence ($_{37}$LFPTSTSLSPFYLRPPSF$_{54}$), three α crystallin core domain sequences [$_{75}$FSVNLDVK$_{82}$ (β3), $_{131}$LTITSSLS$_{138}$ (β8), and $_{141}$GVLTVNGP$_{148}$ (β9)], and the C-terminal sequence ($_{155}$PERTIPITREEK$_{166}$) were identified as subunit−subunit interaction sites in αB crystallin. The pin array studies confirmed and expanded on spectroscopic observations, mutational studies, proteolytic degradation experiments, and a two-hybrid screen that characterized interactive domains in sHSPs. The subunit−subunit interactive domains identified by the pin arrays were consistent with the dimer and complex interfaces (β3, β8, β9, and the I-X-I/V motif) identified in the crystal structures of Mj sHSP16.5 and wheat sHSP16.9 with one exception. The pin arrays did not identify sequences in the loop region connecting β5 and β7 as interactive sequences for dimerization in αB crystallin (*39*, *45*, *47*). In separate reports using peptide scanning techniques, sequences for subunit−subunit assembly and chaperone function were identified in αB crystallin and a small heat shock protein, sHSPB, that were consistent with the sequences identified by the pin arrays (*47*, *50*, *51*). A sequence in the α crystallin core domain of αA crystallin, KFVIFLDVKHFSPEDLTVK which is homologous to the sequence $_{75}$FSVNLDVK$_{82}$ from the α crystallin core domain of human αB crystallin, was reported to have chaperone-like activity in vitro (*52*).

In this report, protein pin arrays identified and characterized interactive sequences that were mapped to a three-dimensional (3D) structural model. Seven interactive domains for chaperone function in human αB crystallin were identified as sequences that interacted with denatured β_H crystallin, γD crystallin, alcohol dehydrogenase, and citrate synthase. Two of the interactive peptides, $_{73}$DRFSVNLDVKHFS$_{85}$ and $_{131}$LTITSSLSDGV$_{141}$, were synthesized and observed to have chaperone activity in vitro against the thermal aggregation of β_H crystallin, ADH, and CS. The seven interactive sequences for chaperone function identified by the pin arrays overlapped with the interactive domains for subunit−subunit interactions and complex assembly identified previously (*47*). Taken together, these data suggest that interactive domains in αB crystallin mediate dual functions of chaperone activity and subunit−subunit assembly.

MATERIALS AND METHODS

Synthesis of Pins, Binding, and Detection of Peptides Binding to Ligand Proteins. The αB crystallin protein pin array was used to measure the extent of interaction between peptides and chaperone target proteins, including bovine β_H crystallin, human γD crystallin, equine alcohol dehydrogenase (ADH), and porcine citrate synthase (CS) as described previously (Figure 1) (*47*). The purities of the target proteins used in the pin array assays, bovine β_H crystallin, human γD crystallin, equine alcohol dehydrogenase (ADH), and porcine citrate synthase (CS), were determined to be >90% by SDS−PAGE. In addition, primary antibodies for each target protein were specific to that target protein, and consequently, contaminating proteins that may bind to the

Table 1: List of Proteins and Antibodies Used in the Protein Pin Array Assays[a]

protein	catalog no.	supplier	amount of protein used/well
bovine β_H crystallin	SPP-235	Stressgen Inc. (Victoria, BC)	0.05 μmol
human γD crystallin	recombinant, purified		0.05 μmol
equine alcohol dehydrogenase	05646	Sigma-Aldrich (St. Louis, MO)	0.05 μmol
porcine citrate synthase	103381	Roche Diagnostics (Indianapolis, IN)	0.05 μmol

antibody	catalog No.	supplier	dilution
mouse anti-β crystallin	SPA-230	Stressgen Inc.	1:1000
mouse anti-γ crystallin	Custom		1:1000
rabbit anti-alcohol dehydrogenase	AB1202	Chemicon International (Temecula, CA)	1:40000
mouse anti-citrate synthase	RDI−CBL 249	RDI Diagnostics Inc.	1:1000

[a] Column 1 lists the name of the purchased or synthesized protein or antibody. Column 2 lists the catalog number of the purchased or synthesized protein or antibody. Column 3 lists the supplier of the purchased protein or antibody. Column 4 lists the concentration of the protein or antibody used in the pin array assay.

peptides will not be detected. Eighty-four sequential and overlapping peptide fragments corresponding to residues 1−175 of human αB crystallin were synthesized employing a simultaneous peptide synthesis strategy developed by Geysen, called multipin peptide synthesis (Mimotopes, San Diego, CA) (*53*, *54*). Peptides were immobilized on derivatized polyethylene pins arranged in a microtiter ELISA plate format. Each peptide was eight amino acids in length, and consecutive peptides were offset by two amino acids. All peptides were bound covalently to the surface of the plastic pins. The first peptide was $_1$MDIAIHHP$_8$ and the last peptide $_{168}$PAVTAAPK$_{175}$ for human αB crystallin. All proteins and antibodies were purchased from suppliers as listed in Table 1.

Human myoglobin did not interact with the αB crystallin peptides and was the negative control for the protein pin array assay (*47*). Positive interactions resulted in the blue color in the wells of the ELISA plate. The intensity of the blue color in the wells was measured at 450 nm using an ELISA plate reader (BioTek, Winooski, VT). The intensity of the blue color (plotted on the *X*-axis) was a measure of the level of interaction between αB crystallin peptides (plotted on the *Y*-axis) and target proteins. To measure the effect of temperature on the interactions between interactive peptides and the target proteins, the target proteins were heated in a water bath at 45 °C for 15 min prior to use. Pin arrays are unable to differentiate between monomers, dimers, or oligomers of target proteins that exist in solution. Instead, pin arrays are very sensitive detectors of interactions between individual peptides and the entire population (monomers, dimers, or oligomers) of specific target proteins that may exist in solution under specific conditions. Each target protein was assayed two to five times. A single pin array was used for all experiments, and no change in interactions was observed after more than 30 repetitions. The last three peptides of the protein pin array, $_{163}$REEKPAVT$_{170}$, $_{165}$EKPAVTAA$_{172}$, and $_{167}$PAVTAAPK$_{174}$, correspond to the epitope ($_{163}$REEKPAVTAAPKK$_{175}$) recognized by the primary antibody for human αB crystallin. A positive reaction is observed for these three peptides in the absence of human αB crystallin as the ligand due to direct binding of the anti-human αB crystallin antibody to these three peptides. The loss of efficiency for the pin array was measured using this assay. The loss of efficiency for the pin array was determined to be <5% after more than 30 assays.

Molecular Modeling of Human αB Crystallin. The homology modeling program Molecular Operating Environment (MOE) (Chemical Computing Group, Inc., Montreal, PQ) was used to construct the 3D homology model of human αB crystallin as described previously (*47*). The software included modules for multiple-sequence alignment, structure superposition, contact analysis, fold identification, analysis of the stereochemical quality of the predicted models which takes into account parameters such as planarity, chirality, ϕ and ψ preferences, χ angles, nonbonded contact distances, and unsatisfied donors and acceptors (*55*). The wheat sHSP16.9 crystal structure was chosen as the template for the homology modeling of human αB crystallin because the sequence of wheat sHSP16.9 is most similar with that of human αB crystallin (40% in the α crystallin core domain and 25.4% overall) of all the available crystal structures of sHSPs. In building the homology model of human αB crystallin, the primary sequence of human αB crystallin was aligned with the template protein, wheat sHSP16.9 primary sequence using ClustalX (*56*, *57*). The predicted secondary structure of human αB crystallin was then obtained (JPred) and verified with the available spin labeling information for the structural elements (*58*). The secondary structure of human αB crystallin was then aligned structurally with the observed secondary structure of wheat sHSP16.9. This alignment was used to create a series of 10 energy-minimized models in MOE. Each model was evaluated using the ModelEval module of MOE, and the best fit was selected as the final model and verified with Procheck (*59*). The αB crystallin 3D model computed on the basis of the X-ray crystal structures of wheat sHSP16.9 and Mj sHSP16.5 was consistent with the electron spin resonance (ESR) data and previous homology models of αB crystallin (*58*, *60*−*63*). When the 3D homology model of αB crystallin was superimposed on the crystal structures of wheat sHSP16.9 and Mj sHSP16.5, the Cα root-mean-square deviation of the fit was 3.25 Å (*47*). Superimposition of the conserved α crystallin core domains of the three structures resulted in a Cα root-mean-square deviation of 2.06 Å. Hydrophobic surface areas formed by the chaperone sequences were calculated by a custom script provided by the manufacturer (Chemical Computing Group, Inc.). Graphical representations of human αB crystallin were made using PyMol and MOE.

RESULTS

Interactive Sites for β_H and γD Crystallin in αB Crystallin. Protein pin arrays enabled the identification of interactive sequences necessary for the chaperone activity of human αB crystallin. Interactions between immobilized 8-mer human

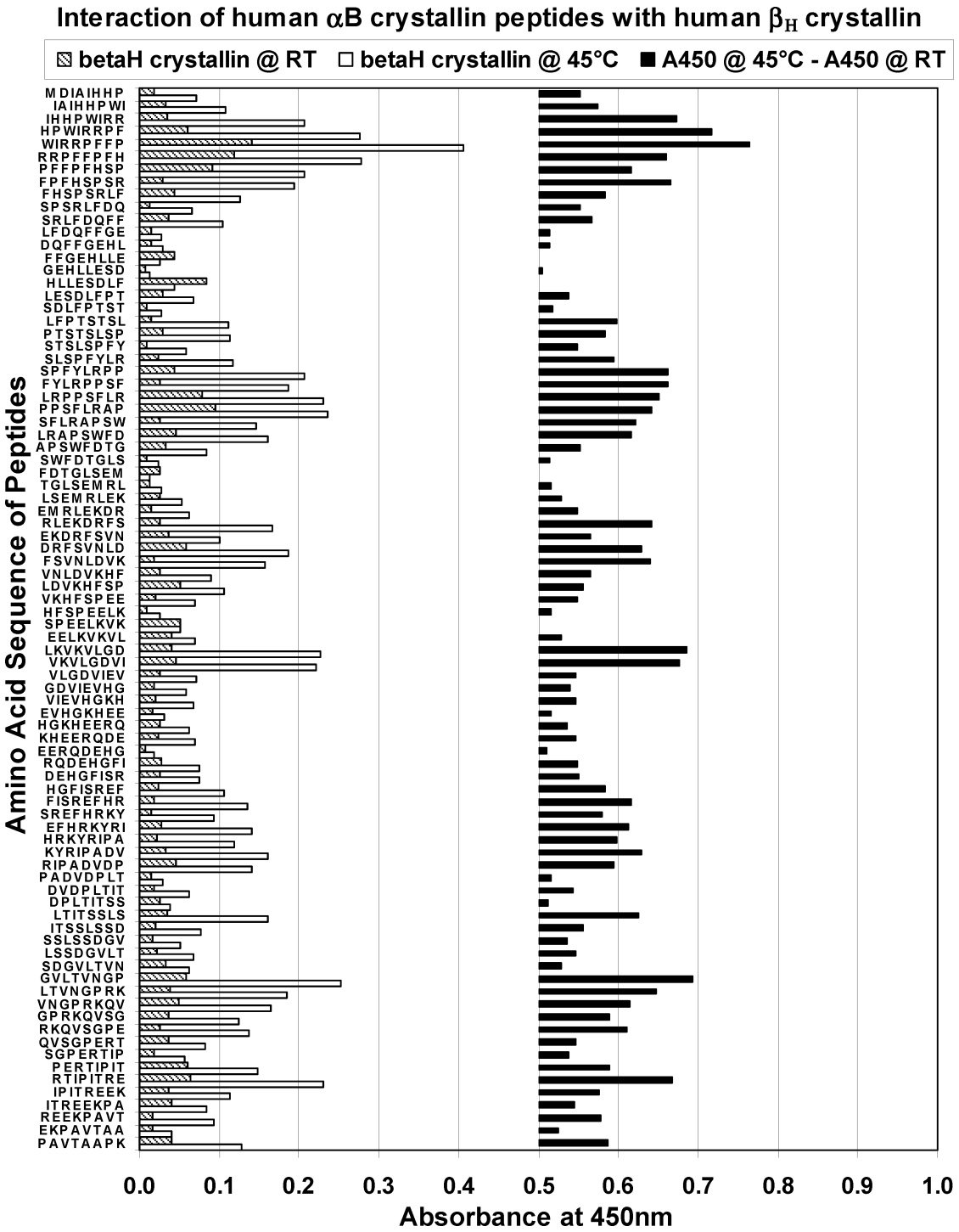

FIGURE 2: Pattern of interactions between human αB crystallin 8-mer peptides immobilized on pins and unheated β_H crystallin at 23 °C and β_H crystallin preheated at 45 °C for 15 min. The amino acid sequences of each 8-mer human αB crystallin peptide immobilized sequentially on 84 pins in a 96-well ELISA plate format are listed on the *Y*-axis. The absorbances measured at 450 nm for the interactions between the αB crystallin peptides and unheated β_H crystallin (striped bars) or preheated β_H crystallin (white bars) using an ELISA-based colorimetric method are listed on the primary *X*-axis. The length of the bars is proportional to the strength of the interaction of that peptide with unheated or preheated human β_H crystallin (the longer the bar, the stronger the interaction). Interactions were not observed at every peptide, and there were distinct patterns of interactions with both unheated and preheated β_H crystallin. An absorbance value of <0.134 with preheated β_H crystallin was considered the baseline for nonspecific interactions. The interaction of the majority of peptides (56 of 84) was stronger with preheated β_H crystallin than with unheated β_H crystallin. The difference in the measured absorbance (A_{450}@45 °C − A_{450}@RT) for each peptide represents the increased or decreased level of interaction of that peptide with preheated human β_H crystallin relative to unheated β_H crystallin (plotted to the right as black bars). Overall, the interaction between αB crystallin peptides was stronger with preheated β_H crystallin than with unheated β_H crystallin.

αB crystallin peptides and unheated and preheated β_H crystallin, a natural protein constituent of lens cells, were assessed as absorbances at 450 nm (λ) and 23 °C. Maximum absorbances were measured for the peptide sequences $_{9}$WIRRPFFP$_{16}$, $_{45}$SPFYLRPP$_{52}$, $_{47}$FYLRPPSF$_{54}$, $_{51}$PPSFLRAP$_{58}$, $_{69}$RLEKDRFS$_{76}$, $_{75}$FSVNLDVK$_{82}$, $_{89}$LKVKVLGD$_{96}$, $_{113}$FISREFHR$_{120}$, $_{121}$KYRIPADV$_{128}$, $_{131}$LTITSSLS$_{138}$, $_{141}$GVLTVNGP$_{148}$, and $_{157}$RTIPITRE$_{164}$ when unheated β_H crys-

Table 2: List of αB Crystallin Peptides that Recorded the Highest Absorbances in the Presence of Unheated and Preheated β_H Crystallin, γD Crystallin, ADH, and CS[a]

region	β_H crystallin	γD crystallin	ADH	CS	common
N-terminus		$_{3}$IAIHHPWI$_{10}$			
N-terminus	**$_{9}$WIRRPFFP$_{16}$**	**$_{9}$WIRRPFFP$_{16}$**	**$_{9}$WIRRPFFP$_{16}$**	**$_{9}$WIRRPFFP$_{16}$**	$_{9}$WIRRPFFPFHSP$_{20}$
N-terminus		$_{21}$PFFPFHSP$_{28}$	$_{21}$PFFPFHSP$_{28}$	$_{23}$FPFHSPSR$_{30}$	
N-terminus		$_{25}$DQFFGEHL$_{32}$	$_{27}$FFGEHLLE$_{34}$		
N-terminus			$_{37}$LFPTSTSL$_{44}$		
N-terminus	$_{45}$SPFYLRPP$_{52}$	$_{43}$SLSPFYLR$_{50}$	$_{43}$SLSPFYLR$_{50}$	$_{43}$SLSPFYLR$_{50}$	$_{43}$SLSPFYLRPPSFLRAP$_{58}$
N-terminus	$_{47}$FYLRPPSF$_{54}$	$_{47}$FYLRPPSF$_{54}$	$_{49}$LRPPSFLR$_{56}$	$_{47}$FYLRPPSF$_{54}$	
N-terminus	$_{51}$PPSFLRAP$_{58}$	$_{53}$SFLRAPSW$_{60}$		$_{55}$LRAPSWFD$_{62}$	
core domain	$_{69}$RLEKDRFS$_{76}$		$_{69}$RLEKDRFS$_{76}$		
core domain	**$_{75}$FSVNLDVK$_{82}$**	**$_{75}$FSVNLDVK$_{82}$**	**$_{75}$FSVNLDVK$_{82}$**	**$_{75}$FSVNLDVK$_{82}$**	$_{75}$FSVNLDVK$_{82}$
core domain	$_{89}$LKVKVLGD$_{96}$				
core domain	$_{113}$FISREFHR$_{120}$	$_{111}$HGFISREF$_{118}$		$_{113}$FISREFHR$_{120}$	$_{113}$FISREFHR$_{120}$
core domain	$_{121}$KYRIPADV$_{128}$	$_{117}$EFHRKYRI$_{124}$	$_{115}$SREFHRKY$_{122}$		
core domain	**$_{131}$LTITSSLS$_{138}$**	**$_{131}$LTITSSLS$_{138}$**	**$_{131}$LTITSSLS$_{138}$**	**$_{131}$LTITSSLS$_{138}$**	$_{131}$LTITSSLS$_{138}$
core domain	$_{141}$GVLTVNGP$_{148}$	$_{141}$GVLTVNGP$_{148}$	$_{141}$GVLTVNGP$_{148}$	$_{143}$LTVNGPRK$_{150}$	$_{141}$GVLTVNGP$_{148}$
C-terminus	$_{157}$RTIPITRE$_{164}$		$_{157}$RTIPITRE$_{164}$	$_{157}$RTIPITRE$_{164}$	$_{157}$RTIPITRE$_{164}$

[a] Column 1 lists the region of αB crystallin where each chaperone sequence is located. Column 2 lists the interactive sequences in αB crystallin for human β_H crystallin. Column 3 lists the interactive sequences in αB crystallin for human γD crystallin. Column 4 lists the αB crystallin peptide chaperone sequences for ADH. Column 5 lists the αB crystallin peptide chaperone sequences for CS. Column 6 lists the seven common chaperone sequences that were observed to interact with three or more preheated chaperone target proteins.

tallin was the target protein (Figure 2, striped bars). Similar absorbance maxima were measured for interactions between αB crystallin peptides and β_H crystallin that was preheated at 45 °C for 15 min (Figure 2, white bars). αB crystallin peptides that had positive interactions with unheated and preheated β_H crystallin were identical and differed only in the magnitude of the observed absorbances (Figure 2, black bars). For all sequences in the pin array, 80 of 84 αB crystallin peptides had higher absorbances with preheated β_H crystallin than with unheated β_H crystallin (A_{450}@45 °C − A_{450}@23 °C > 0), while the absorbances of the remaining four peptides were similar for preheated and unheated β_H crystallin (A_{450}@45 °C − A_{450}@23 °C ∼ 0). Peptides with maximum absorbance were flanked on either side by one or two overlapping peptides with lower absorbances giving the appearance of a peak. The overlapping flanking peptides were shifted toward the N- or C-termini by two amino acids from the peptide recording the maximum absorbance. Peptides with the maximum difference in the magnitude of absorbance (A_{450}@45 °C − A_{450}@23 °C) in each peak are listed in column 2 of Table 2. Far-UV CD spectroscopy indicated that the loss of secondary structure of β_H crystallin upon heating at 45 °C for 15 min was <10%, and the ellipticity value of the major absorption peaks in the near-UV CD spectrum of preheated β_H crystallin decreased by less than 20% (Figures 4a and 5a).

When β_H crystallin was replaced with γD crystallin, a native protein constituent of lens cytoplasm from the same gene family as the β crystallins, as the ligand in the pin array, 12 interactive sequences were identified (Figure 3, striped bars). The 12 peptides that recorded maximum absorbances at 450 nm (λ) with unheated γD crystallin were $_{3}$IAIHHPWI$_{10}$, $_{9}$WIRRPFFP$_{16}$, $_{21}$PFFPFHSP$_{28}$, $_{25}$DQFFGEHL$_{32}$, $_{43}$SLSPFYLR$_{50}$, $_{47}$FYLRPPSF$_{54}$, $_{52}$SFLRAPSW$_{59}$, $_{75}$FSVNLDVK$_{82}$, $_{111}$HGFISREF$_{118}$, $_{117}$EFHRKYRI$_{124}$, $_{131}$LTITSSLS$_{138}$, and $_{141}$GVLTVNGP$_{148}$. Maximum absorbances were measured at similar peptide sequences in αB crystallin when γD crystallin was preheated at 45 °C for 15 min (Figure 3, white bars). The magnitude of the absorbances was higher at 56 of 84 αB crystallin peptides (Figure 3, black bars) and lower at 16 of the 84 peptides when γD crystallin was preheated at 45 °C for 15 min. The measured absorbances for the remaining 12 peptides were similar in magnitude for both unheated and preheated γD crystallin. αB crystallin peptides that had the highest absorbances with unheated or preheated γD crystallin were flanked on either side by one or two overlapping peptides with lower absorbances giving the appearance of a peak. The overlapping flanking peptides were shifted toward the N- or C-termini by two amino acids from the peptide recording the maximum absorbance. Peptides with the maximum difference in magnitude of absorbance (A_{450}@45 °C − A_{450}@23 °C) in each peak were listed in column 3 of Table 2. Far-UV CD spectroscopy indicated that the loss of secondary structure of γD crystallin upon heating at 45 °C for 15 min was <10%, and the ellipticity value of the major absorption peaks in the near-UV CD spectrum of preheated γD crystallin decreased by less than 25% (Figures 4b and 5b).

Chaperone Sites for ADH and CS in **α***B Crystallin.* In addition to interactions with physiological target proteins in the β/γ crystallin family, interactions of the αB crystallin peptides with unheated and preheated chaperone target proteins, alcohol dehydrogenase (ADH), and citrate synthase (CS) were assessed. Prior to use in the pin array assay, the secondary structures of β_H crystallin, γD crystallin, ADH, and CS were determined using far-ultraviolet circular dichroism (UV CD) at 23 °C, after heating at 45 °C for 15 min and after heating at 50 °C for 60 min (Figure 4). The maximum ellipticity (Θ_{max}) for β_H crystallin was observed to be at 214 nm (λ) at all three temperatures, and the magnitude of the maximum ellipticity (Θ_{max}) decreased from −5576 deg cm^2 dmol^{-1} at 23 °C to −5043 deg cm^2 dmol^{-1} after heating at 45 °C for 15 min and to −4501 deg cm^2 dmol^{-1} after heating at 50 °C for 60 min (Figure 4a). Similarly, the Θ_{max} for γD crystallin was observed to be at 217 nm (λ) at all three temperatures, and the magnitude of Θ_{max} decreased from −5571 deg cm^2 dmol^{-1} at 23 °C to −5150 deg cm^2 dmol^{-1} after heating at 45 °C for 15 min and to −4719 deg cm^2 dmol^{-1} after heating at 50 °C for 60 min (Figure 4b). The Θ_{max} for ADH was at 215 nm (λ), and the magnitude of the Θ_{max} decreased from −5190 deg cm^2 dmol^{-1} at 23 °C to −5139 deg cm^2 dmol^{-1} after heating at

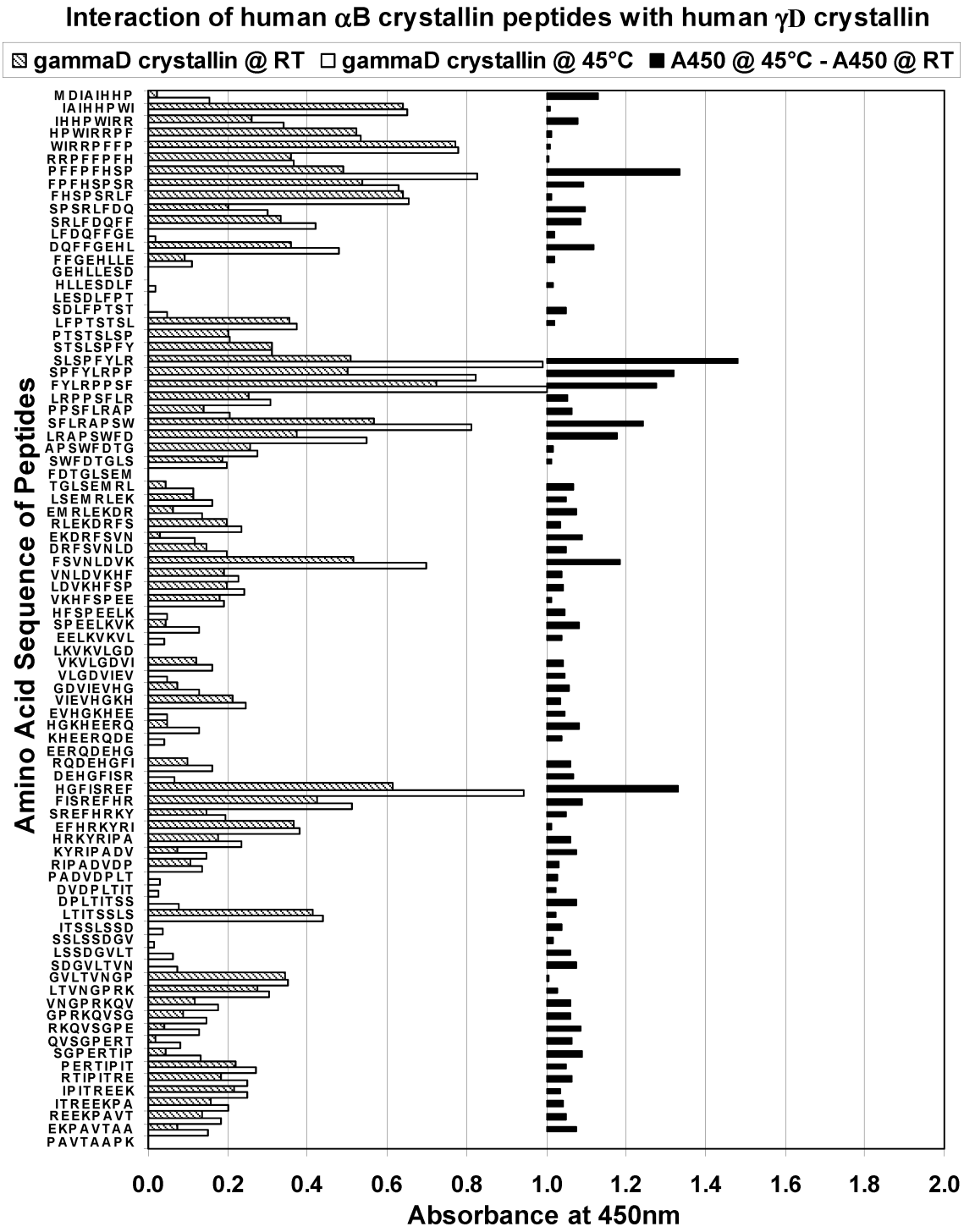

FIGURE 3: Pattern of interactions between human αB crystallin 8-mer peptides immobilized on pins and unheated γD crystallin at 23 °C and γD crystallin preheated at 45 °C for 15 min. The amino acid sequences of each 8-mer human αB crystallin peptide immobilized sequentially on 84 pins in a 96-well ELISA plate format are listed on the *Y*-axis. The absorbances measured at 450 nm for the interactions between the αB crystallin peptides and unheated γD crystallin (striped bars) or preheated γD crystallin (white bars) using an ELISA-based colorimetric method are listed on the primary *X*-axis. The length of the bars is proportional to the strength of the interaction of that peptide with unheated or preheated human γD crystallin. Interactions were not observed at every peptide, and there were distinct patterns of interactions with both unheated and preheated γD crystallin. An absorbance value of <0.348 with preheated γD crystallin was considered the baseline for nonspecific interactions. The interaction of the majority of peptides (56 of 84) was stronger with preheated γD crystallin than with unheated γD crystallin. The difference in the measured absorbance (A_{450}@45 °C − A_{450}@RT) for each peptide represents the increased or decreased level of interaction of that peptide with preheated human γD crystallin relative to unheated γD crystallin (plotted on the right as black bars). Overall, the interaction between αB crystallin peptides was stronger with preheated γD crystallin than with unheated γD crystallin.

45 °C for 15 min, indicating a <1% loss of secondary structure upon heating at 45 °C (Figure 4c). The magnitude of the Θ_{max} of ADH further decreased to −2523 deg cm^2 dmol^{-1} after heating at 50 °C for 60 min, indicating a >50% loss of secondary structure upon heating at 50 °C (Figure 4c). The Θ_{max} for CS was at 215 nm (λ), and the magnitude of the Θ_{max} decreased from −13076 deg cm^2 dmol^{-1} at 23 °C to −11070 deg cm^2 dmol^{-1} after heating at 45 °C for 15

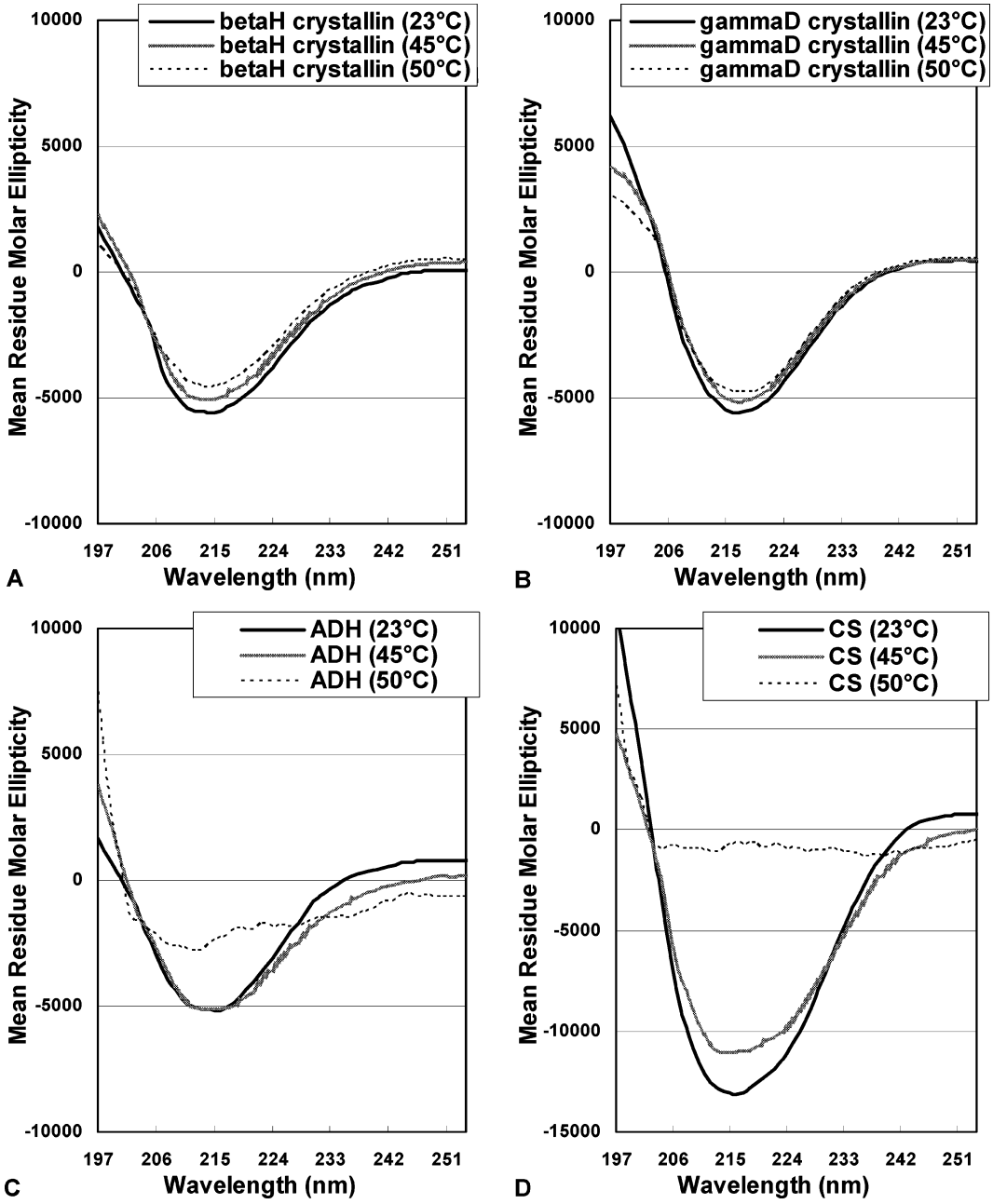

FIGURE 4: Far-UV CD of β_H crystallin, γD crystallin, alcohol dehydrogenase (ADH), and citrate synthase (CS). Spectra were collected for β_H crystallin (A), γD crystallin (B), ADH (C), and CS (D), at 23, 45, and 50 °C. The UV CD spectra of β_H and γD crystallin remained largely unchanged between 23 and 50 °C (*83*, *84*). The spectra for ADH at 23 and 45 °C were similar, while at 50 °C, there was a significant decrease in the ellipticity at 215 nm. The spectra for CS showed decreased ellipticity at 215 nm with an increase in temperature from 23 to 50 °C. Far-UV CD spectra indicated that β_H crystallin and γD crystallin were thermostable and remained folded up to 50 °C and ADH remained folded up to 45 °C but unfolded at 50 °C. CS was the least thermostable of the four chaperone target proteins and unfolded at 45 °C. The amount of unfolding in response to the increase in temperature was as follows: CS $\gg$ ADH $>$ β_H crystallin $\sim$ γD crystallin.

min, indicating an ~15% loss of secondary structure upon heating at 45 °C (Figure 4d). When CS was heated at 50 °C for 60 min, the Θ_{max} of CS decreased to −648 deg cm^2 dmol^{-1}, indicating a >95% loss of secondary structure at 50 °C (Figure 4d).

Prior to use in the pin array assay, the tertiary structures of β_H crystallin, γD crystallin, ADH, and CS were determined using near-ultraviolet circular dichroism at 23 °C, after heating at 45 °C for 15 min and after heating at 50 °C for 60 min (Figure 5). The maximum absorption peak for β_H crystallin was at 267 nm (λ) at 23 °C. The magnitude of the absorption peak at 267 nm (λ) decreased from 30.71 deg cm^2 dmol^{-1} at 23 °C to 24.22 deg cm^2 dmol^{-1} upon heating β_H crystallin at 45 °C for 15 min, indicating partial unfolding at 45 °C, and to 15.78 deg cm^2 dmol^{-1} upon heating at 50 °C for 60 min, indicating substantial unfolding at 50 °C (Figure 5a). The maximum absorption peak for γD crystallin was at 269 nm (λ) at 23 °C. The magnitude of the absorption peak at 269 nm (λ) decreased from 17.26 deg cm^2 dmol^{-1} at 23 °C to 12.74 deg cm^2 dmol^{-1} upon heating γD crystallin at 45 °C for 15 min, indicating partial unfolding at 45 °C, and to 6.75 deg cm^2 dmol^{-1} upon heating at 50 °C for 60 min, indicating substantial unfolding at 50 °C (Figure 5b). The maximum absorption peak for ADH was at 270 nm (λ)

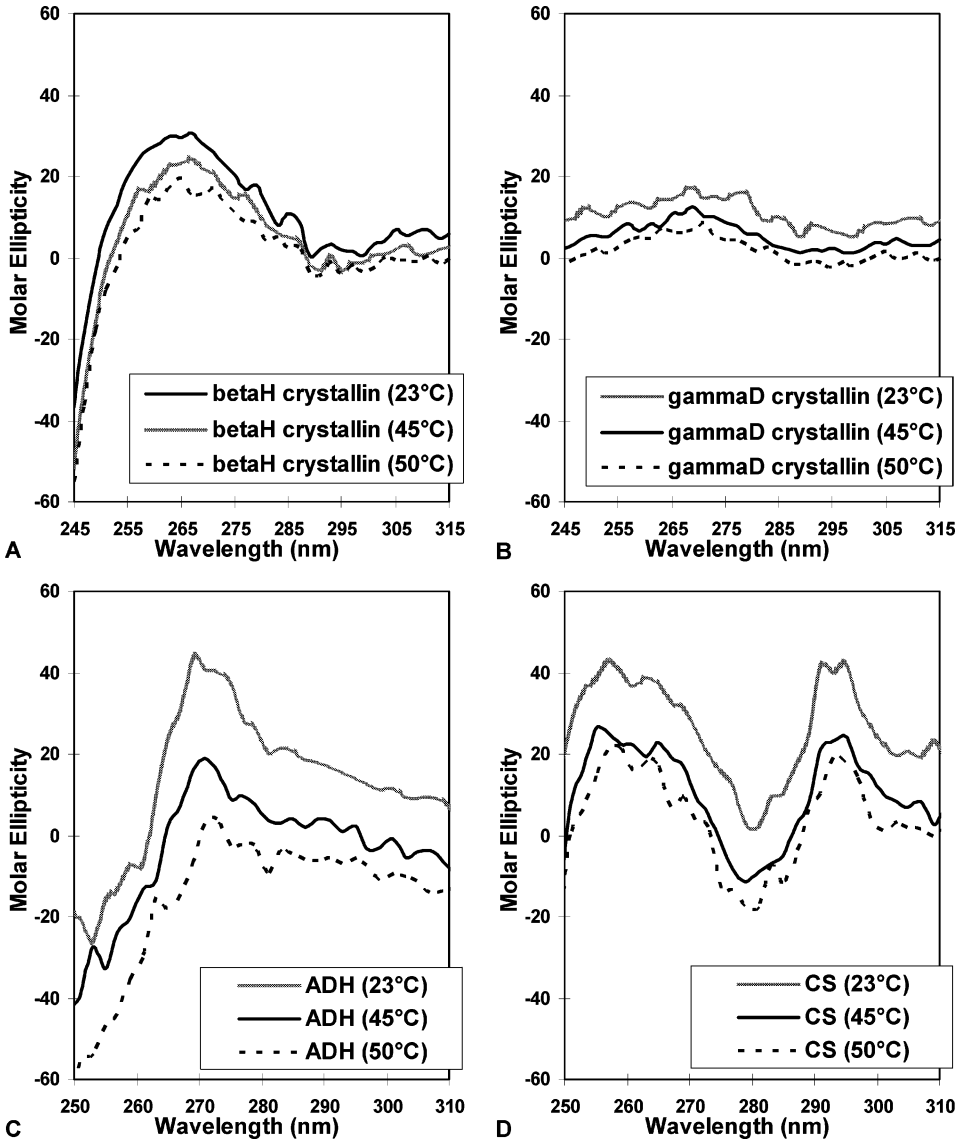

FIGURE 5: Near-UV CD of β_H crystallin, γD crystallin, ADH, and CS. Spectra were collected for β_H crystallin (A), γD crystallin (B), ADH (C), and CS (D) at 23, 45, and 50 °C. The ellipticity of the absorption peaks in the near-UV CD spectra of β_H crystallin, γD crystallin, ADH, and CS decreased by 20−60% upon heating at 45 °C for 15 min.

at 23 °C. The magnitude of the absorption peak at 270 nm (λ) decreased from 44.27 deg cm^2 dmol^{-1} at 23 °C to 14.23 deg cm^2 dmol^{-1} upon heating ADH at 45 °C for 15 min, indicating partial unfolding at 45 °C, and to −2.37 deg cm^2 dmol^{-1} upon heating at 50 °C for 60 min, indicating substantial unfolding at 50 °C (Figure 5c). The maximum absorption peak for CS was at 257 nm (λ) at 23 °C. The magnitude of the absorption peak decreased at 257 nm (λ) from 42.54 deg cm^2 dmol^{-1} at 23 °C to 25.20 deg cm^2 dmol^{-1} upon heating CS at 45 °C for 15 min, indicating partial unfolding at 45 °C, and to 20.95 deg cm^2 dmol^{-1} upon heating at 50 °C for 60 min, indicating substantial unfolding at 50 °C (Figure 5d).

The pattern of absorbance at 450 nm (λ) when αB crystallin peptides were assayed with unheated and preheated ADH was similar to the absorbance pattern obtained with unheated and preheated β_H/γD crystallin (Figure 6). Maximum absorbances were measured for the αB crystallin peptide sequences $_{9}$WIRRPFFP$_{16}$, $_{13}$PFFPFHSP$_{20}$, $_{27}$FFGEHLLE$_{34}$, $_{37}$LFPTSTSL$_{44}$, $_{43}$SLSPFYLR$_{50}$, $_{48}$LRPPSFLR$_{55}$, $_{69}$RLEKDRFS$_{76}$, $_{75}$FSVNLDVK$_{82}$, $_{115}$SREFHRKY$_{122}$, $_{131}$LTITSSLS$_{138}$, $_{141}$GVLTVNGP$_{148}$, and $_{157}$RTIPITRE$_{164}$ when ADH was used as the ligand in the pin array assay. The absorbance for 34 of the 84 peptides increased when ADH was preheated at 45 °C for 15 min (A_{450}@45 °C − A_{450}@23 °C > 0), while the absorbance for the remaining 50 peptides was similar for preheated and unheated ADH (A_{450}@45 °C − A_{450}@23 °C ∼ 0). The difference in magnitude of the absorbance of an interactive peptide sequence with preheated and unheated ADH (A_{450}@45 °C − A_{450}@23 °C) was a measure of the increased level of interaction of that peptide with preheated ADH relative to that with unheated native ADH. αB crystallin peptides that had the highest difference in magnitude of absorbances with preheated and unheated ADH (A_{450}@45 °C − A_{450}@23 °C) were flanked on either side by one or two peptides with smaller differences in magnitude of absorbances giving the appearance of peaks. The overlapping flanking peptides were shifted from the peak peptide toward the N- or C-termini by two amino acids from the peptide recording the maximum absorbance. Peptides with the maximum difference in magnitude of absorbance (A_{450}@45 °C − A_{450}@23 °C) in

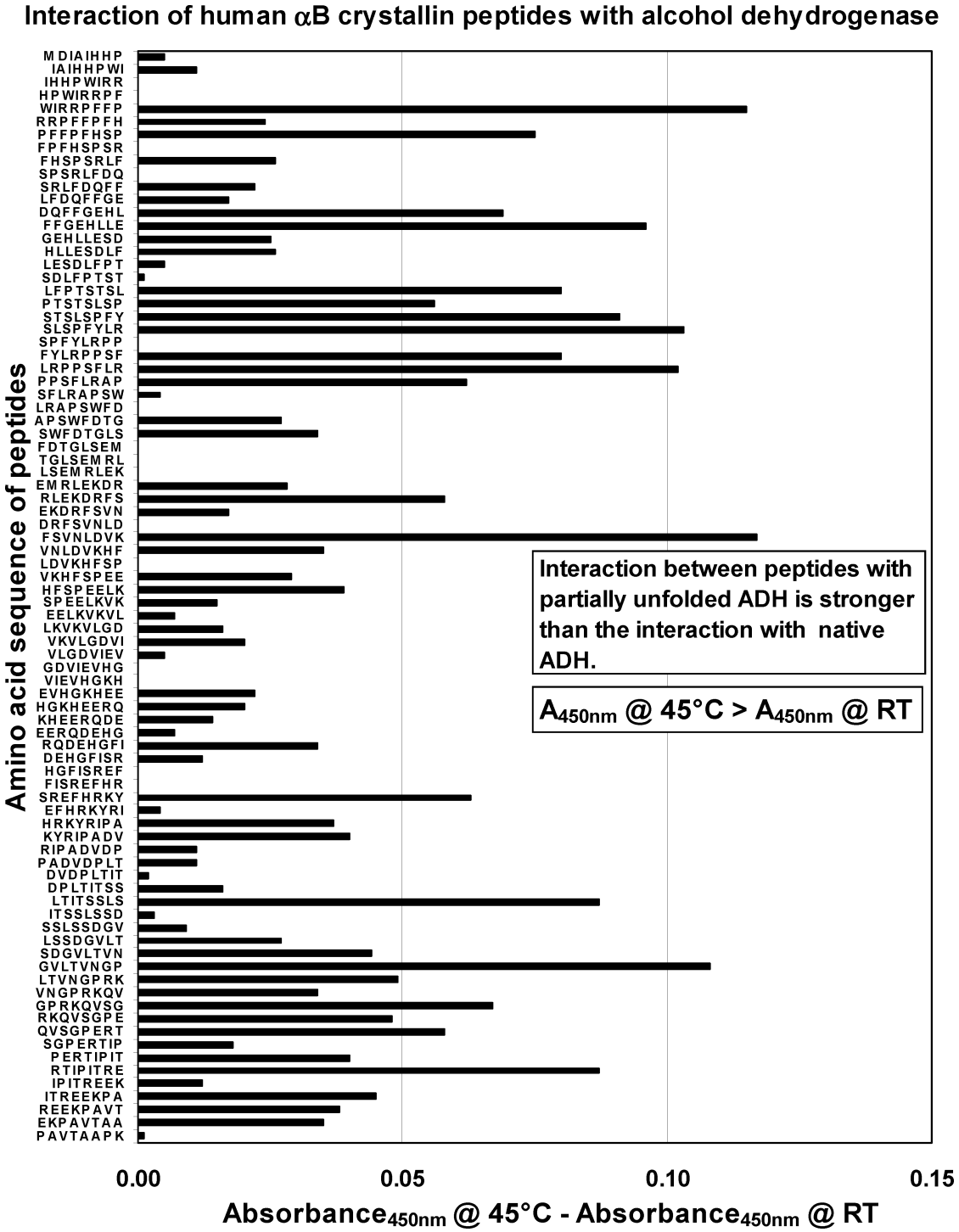

FIGURE 6: Pattern of interaction between human αB crystallin peptides and ADH. The *Y*-axis lists the amino acid sequences of the 8-mer peptides that are immobilized sequentially in a 96-well format. The difference in the measured absorbances of each peptide with preheated partially denatured ADH and unheated native ADH (A_{450}@45 °C − A_{450}@RT) represents an increased or decreased level of interaction of that peptide with partially denatured ADH and native ADH and was represented as a horizontal bar on the *X*-axis. Thirty-four of 84 peptides had a stronger interaction with partially denatured ADH than with native ADH, while the remaining 50 had a similar interaction with either native or partially denatured ADH. The interaction between αB crystallin peptides was stronger with preheated unfolded ADH than with unheated native ADH. An absorbance difference (A_{450}@45 °C − A_{450}@RT < 0.05) was considered the baseline.

each peak were listed in column 4 of Table 2. The results confirmed that the interaction between human αB crystallin was stronger with preheated ADH than with unheated native ADH.

The pattern of absorbance at 450 nm (λ) when αB crystallin peptides were assayed with unheated and preheated CS was similar to the absorbance pattern obtained with unheated and preheated β_H/γD crystallin and ADH (Figure 7). Ten sequences in human αB crystallin ($_{9}$WIRRPFFP$_{16}$, $_{23}$FPFHSPSR$_{30}$, $_{43}$SLSPFYLR$_{50}$, $_{47}$FYLRPPSF$_{54}$, $_{55}$LRAPSWFD$_{62}$, $_{75}$FSVNLDVK$_{82}$, $_{113}$FISREFHR$_{120}$, $_{131}$LTITSSLS$_{138}$, $_{143}$LTVNGPRK$_{150}$, and $_{157}$RTIPITRE$_{164}$) were identified by their absorbance maxima in the presence of CS as the target protein in the pin array assay. αB crystallin peptides that had the highest differences in magnitude of absorbances with preheated and unheated CS (A_{450}@45 °C − A_{450}@23 °C)

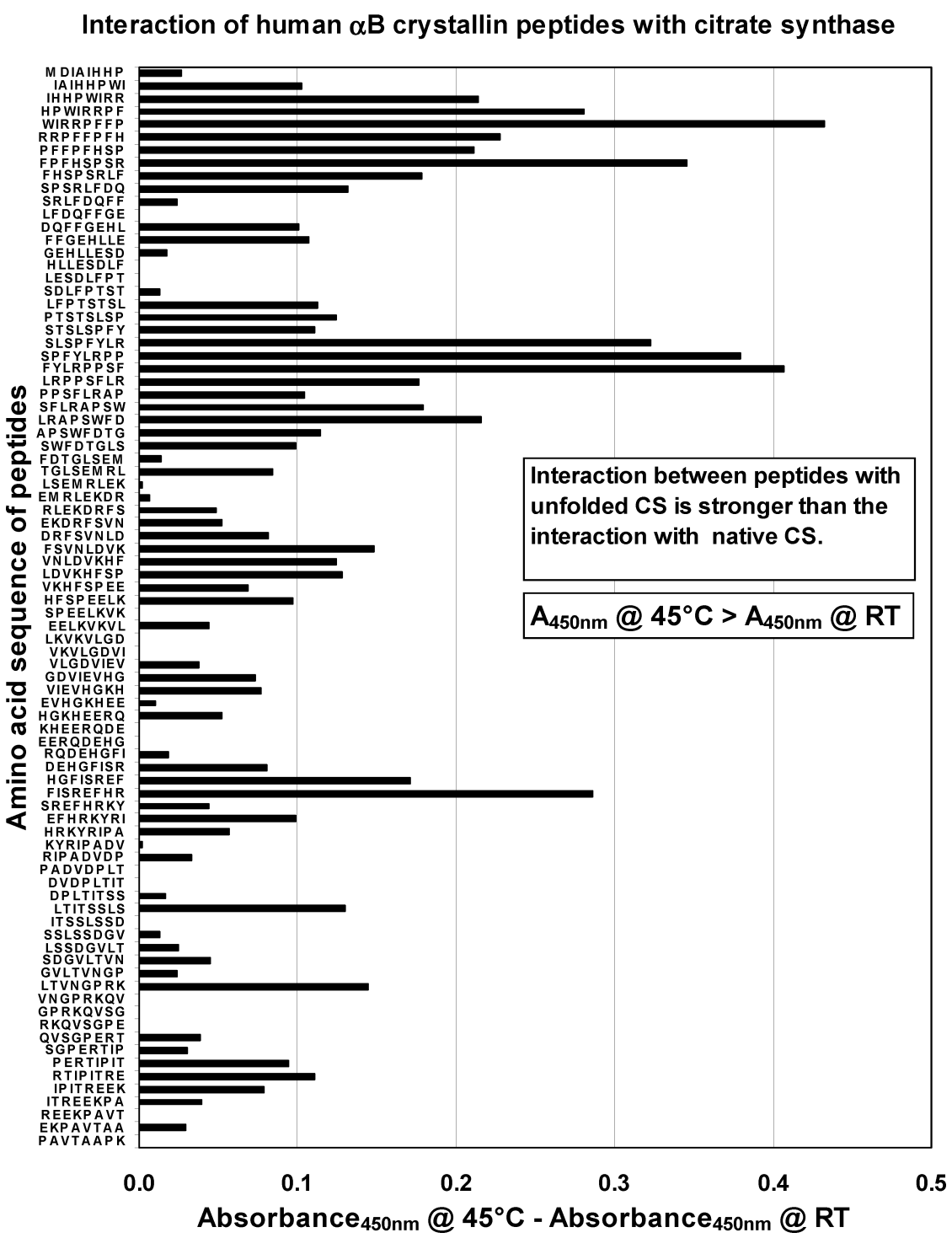

FIGURE 7: Pattern of interaction between human αB crystallin peptides and CS. The *Y*-axis lists the amino acid sequences of the 8-mer peptides that are immobilized sequentially in a 96-well format. The difference in the measured absorbances of each peptide with preheated partially denatured CS and unheated native CS (A_{450}@45 °C − A_{450}@RT) represents an increased or decreased level of interaction of that peptide with preheated partially denatured CS and unheated native CS and was represented as a horizontal bar on the *X*-axis. Seventy-two of 84 peptides had a stronger interaction with partially denatured CS than with native CS, while the remaining 12 had a similar interaction between native and partially denatured CS. The interaction between αB crystallin peptides was stronger with preheated unfolded CS than with unheated native CS. An absorbance difference (A_{450}@45 °C − A_{450}@RT < 0.11) was considered the baseline.

were flanked on either side by one or two peptides with lower differences in magnitude of absorbances giving the appearance of peaks. The overlapping flanking peptides were shifted from the peak peptide toward the N- or C-termini by two amino acids from the peptide recording the maximum absorbance. The difference in magnitude of absorbance for each peptide with partially unfolded and native CS (A_{450}@45 °C − A_{450}@23 °C) represented an increased level of interaction of that peptide with preheated unfolded CS relative to that with unheated native CS. The extent of interaction of 72 of 84 αB crystallin peptides increased when CS was preheated at 45 °C for 15 min (A_{450}@45 °C − A_{450}@23 °C > 0), while the absorbance for the remaining 12 peptides was similar for both native and partially unfolded CS (A_{450}@45 °C − A_{450}@23 °C ∼ 0). Peptides with the maximum difference in magnitude of absorbance (A_{450}@45

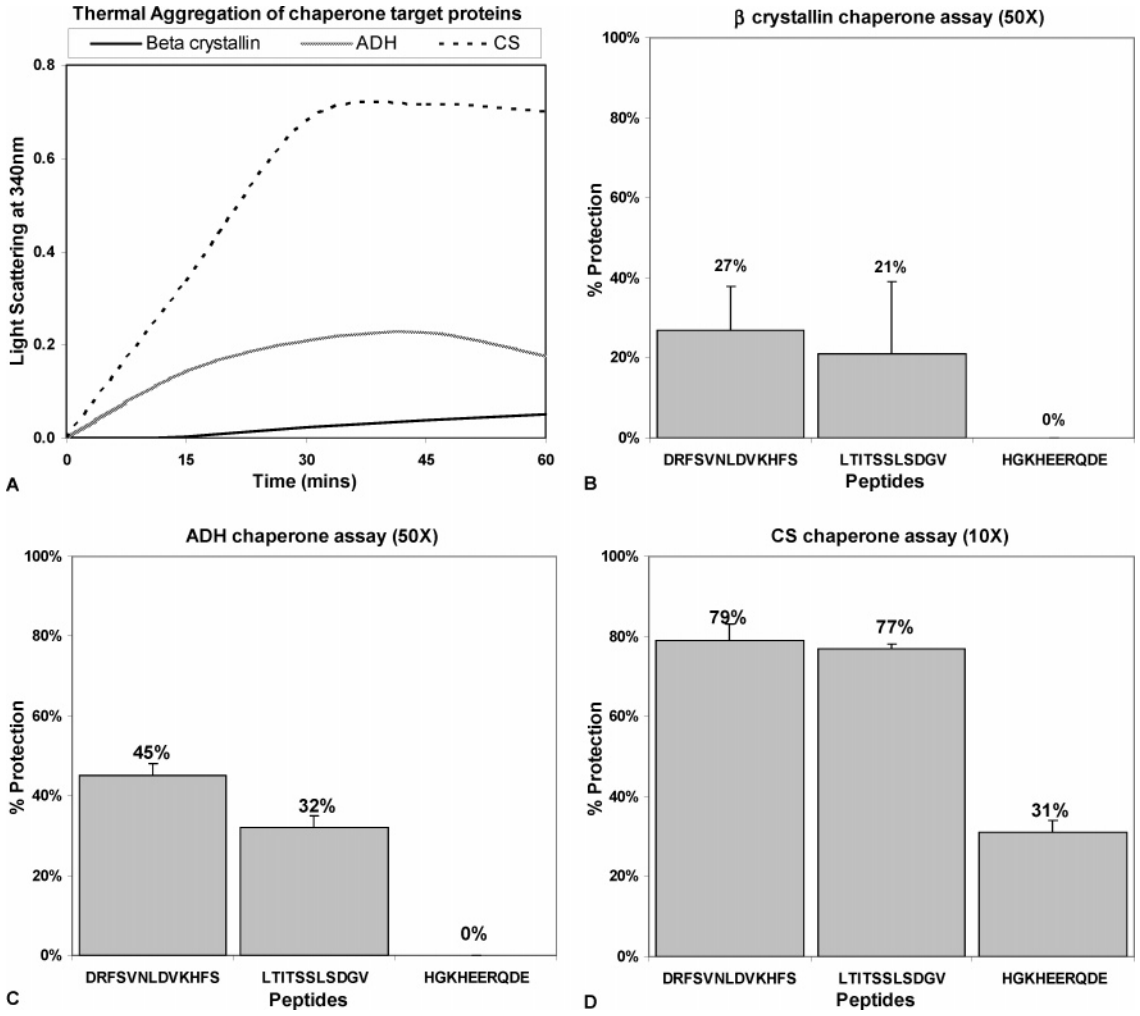

FIGURE 8: Chaperone assays of two positive interactive sequences, $_{73}$DRFSVNLDVKHFS$_{85}$ and $_{131}$LTITSSLSDGV$_{141}$, and a noninteractive sequence, $_{111}$HGKHEERQDE$_{120}$, from the α crystallin core domain of human αB crystallin (control). (A) The extent of thermal aggregation of chaperone target proteins β_H crystallin, ADH, and CS in the absence of peptides was measured as light scattering at 340 nm (λ). Each target protein was heated at 50 °C for 60 min in the absence or presence of one of the peptides. The amount of aggregation correlated with the amount of unfolding observed with near- and far-UV CD. β_H crystallin, the most thermostable of the three proteins, aggregated the least and had an absorbance maximum of 0.05 AU, followed by ADH with an absorbance maximum of 0.23 AU and CS with an absorbance maximum of 0.72 AU in 60 min (unfolding/aggregation, CS > ADH > β_H crystallin). The chaperone activity of each peptide was calculated as the percent protection in which the aggregation of each target protein in the absence of any peptides was set at 0% protection. The ability of the $_{73}$DRFSVNLDVKHFS$_{85}$, $_{131}$LTITSSLSDGV$_{141}$, and $_{111}$HGKHEERQDE$_{120}$ sequences to protect against the thermal aggregation of β_H crystallin (B), ADH (C), and CS (D) was tested in vitro (vertical bars). A 50:1 peptide:target protein molar ratio resulted in modest protection of β_H crystallin and ADH by the two positive peptides, while the control peptide had no protective ability. A 10:1 peptide:target protein molar ratio was sufficient in conferring significant protection against the aggregation of CS by $_{73}$DRFSVNLDVKHFS$_{85}$ and $_{131}$LTITSSLSDGV$_{141}$. The control peptide $_{111}$HGKHEERQDE$_{120}$ conferred partial protection against the aggregation of CS.

°C − A_{450}@23 °C) in each peak were listed in column 5 of Table 2. The increase in the magnitude of the absorbances of the peptides with preheated CS indicated that αB crystallin peptides had a stronger interaction with preheated partially unfolded CS than with unheated native CS.

Seven interactive sequences for chaperone function in αB crystallin ($_9$WIRRPFFPFHSP$_{20}$, $_{43}$SLSPFYLRPPSFLRAP$_{58}$, $_{75}$FSVNLDVK$_{82}$, $_{113}$FISREFHR$_{120}$, $_{131}$LTITSSLS$_{138}$, $_{141}$GV-LTVNGP$_{148}$, and $_{157}$RTIPITRE$_{164}$) were identified as sequences that had the strongest interactions with the model chaperone target proteins, ADH and CS, and the physiological proteins, β_H/γD crystallin, that were preheated at 45 °C for 15 min (column 6 of Table 2). Two of the chaperone sequences are in the N-terminal region, and four are nonoverlapping chaperone sequences in the conserved α crystallin core domain; a single nonoverlapping chaperone sequence is in the C-terminal extension of αB crystallin.

Chaperone Assays of the Interactive Sequences. Two αB crystallin sequences, $_{73}$DRFSVNLDVKHFS$_{85}$ and $_{131}$LTITSSLSDGV$_{141}$, that were in the conserved α crystallin core domain and were observed to have positive interactions with preheated target proteins in the pin array were synthesized to determine their chaperone activity in vitro. The chaperone activity of the peptides was measured as their ability to protect against the thermal aggregation of three chaperone target proteins, β_H crystallin, ADH, and CS, in chaperone assays performed at 50 °C (Figure 8). A noninteractive αB crystallin sequence, $_{111}$HGKHEERQDE$_{120}$, was used as the negative control in the chaperone assays (Figure 8). On the basis of near- and far-UV CD, the three target proteins unfolded in the order CS ≫ ADH ≫ β_H crystallin when they were heated at 50 °C for 60 min (Figures 4 and 5). The extent of thermal aggregation of β_H crystallin, ADH, and CS was measured as light scattering at 340 nm

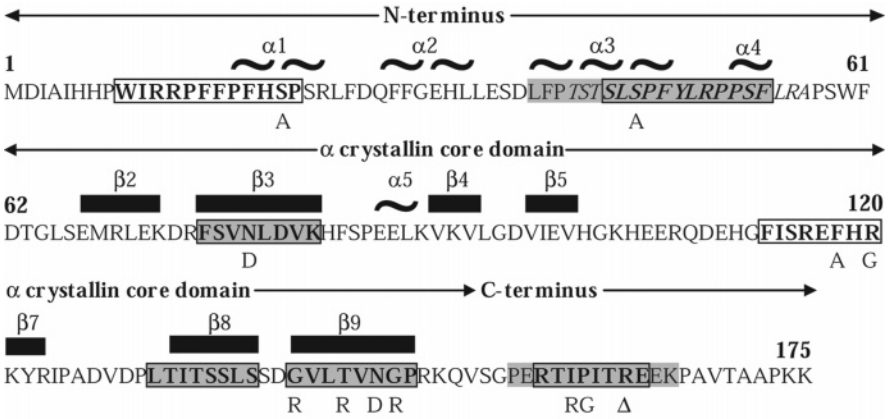

FIGURE 9: Comparison of the peptides identified using the human αB crystallin pin arrays with previously reported interactive sequences for αB crystallin. Sequences identified as interactive domains important for chaperone activity using protein pin arrays are boxed. Subunit−subunit interaction sites identified by the protein pin arrays are highlighted in gray. Site-specific mutations that altered the chaperone function of αB crystallin are shown below the residue(s) that were substituted or deleted (Δ). The secondary structure of αB crystallin predicted by ESR and homology modeling is shown in the form of ∼ symbols which represent helices and ■ symbols which represent β strands (*47*, *60*, *62*). All reported point mutations that were observed to have an effect on the chaperone activity of αB crystallin overlapped with the consensus sequences for chaperone function identified by the pin array assays. The sequence identified by Sreelakshmi et al. (*50*) is shown in italics.

(λ) in the presence and absence of each peptide. The chaperone activity of each peptide was calculated as the percent protection in which the aggregation of each target protein in the absence of any peptides was set at 0% protection (Figure 8). The interactive peptides $_{73}$DRFSVNLDVKHFS$_{85}$ and $_{131}$LTITSSLSDGV$_{141}$ were effective inhibitors of aggregation of all three chaperone target proteins. The greatest protection was observed with CS, the target protein that was the most unfolded upon heating at 50 °C. Less protection was observed with the partially unfolded target proteins, β_H crystallin and ADH. A 50:1 peptide:β_H crystallin/ADH molar ratio resulted in approximately 30% protection for both β_H crystallin and ADH, while a 10:1 peptide:CS molar ratio resulted in greater than 70% protection of CS against thermal aggregation. No protection against aggregation was observed with the control peptide, $_{111}$HGKHEERQDE$_{120}$, even at a 50:1 molar ratio.

Mapping Chaperone Sites to the 3D Structure of Human α*B Crystallin.* The seven sequences identified as interactive domains for chaperone function in human αB crystallin using protein pin arrays (column 6 of Table 1) were assigned secondary structure based on electron spin resonance (ESR) and homology modeling data (Figure 9). $_{9}$WIRRPFFPFHSP$_{20}$ in the N-terminal region, $_{113}$FISREFHR$_{120}$ in the loop region of the α crystallin core domain, and $_{157}$RTIPITRE$_{164}$ in the C-terminal region were unstructured motifs, while $_{43}$SLSPFYLR$_{50}$ (α3) and $_{47}$FYLRPPSF$_{54}$ (α4) formed a helix−turn−helix motif in the N-terminal region. The remaining peptides, $_{75}$FSVNLDVK$_{82}$ (β3), $_{131}$LTITSSLS$_{138}$ (β8), and $_{141}$GVLTVNGP$_{148}$ (β9), formed three β strand motifs in the α crystallin core domain (Figure 9).

The observed interactive domains were mapped to a computed 3D homology model of human αB crystallin to identify the 3D structure of the interactive chaperone sequences (Figure 10a). A space-filling model of the human αB crystallin was generated to view and analyze the interactive domains for the chaperone function in αB crystallin (Figure 10b). The three interactive sequences (β3, β8, and β9) appeared to form one of the external surfaces of the α crystallin core domain, a β sandwich structure resembling an immunoglobulin-like fold, which is characteristic of small heat shock proteins. The β strand residues that were oriented internally stabilized the structure of the β sandwich. Side chains that were oriented externally contributed to the interactions with chaperone target proteins. Residues in the N- and C-termini did not appear to be involved directly in the tertiary structure of the α crystallin core domain. The core domain sequence $_{113}$FISREFHR$_{120}$ formed part of the loop region that connected the two β sheets of the core domain and contributed to its structural integrity. The accessible surface area of the exposed residues of the N-terminal interactive sequences was calculated to be 71% hydrophobic, followed by the C-terminal extension region that was 69% hydrophobic and the α crystallin core domain that was 64% hydrophobic. The proportion of hydrophobic surface over the interactive sequences was consistent with the importance of hydrophobic interactions in the recognition of unfolding proteins by sHSP molecular chaperones (*52*, *64*−*69*).

DISCUSSION

Small heat shock proteins (sHSPs) make up a family of stress proteins and molecular chaperones with molecular masses of up to 43 kDa that contain an N-terminal domain variable in length and primary sequence, a conserved α crystallin core domain, and a C-terminal extension domain that contains the highly conserved I-X-I/V motif. In this report, protein pin arrays identified seven interactive sequences ($_{9}$WIRRPFFPFHSP$_{20}$, $_{43}$SLSPFYLRPPSFLRAP$_{58}$, $_{75}$FSVNLDVK$_{82}$, $_{113}$FISREFHR$_{120}$, $_{131}$LTITSSLS$_{138}$, $_{141}$GVLTVNGP$_{148}$, and $_{157}$RTIPITRE$_{164}$) as being important for the chaperone activity of human αB crystallin using endogenous target proteins β_H/γD crystallins and nonphysiological targets ADH and CS. Although it is possible that interactions of αB crystallin with native β_H crystallin and γD crystallin that require secondary structure might evade detection by the protein pin arrays, it is likely that the pin arrays identified most sequences involved in the interactions of αB crystallin with native β_H crystallin and γD crystallin. The interactive peptides identified by the pin arrays were not the most

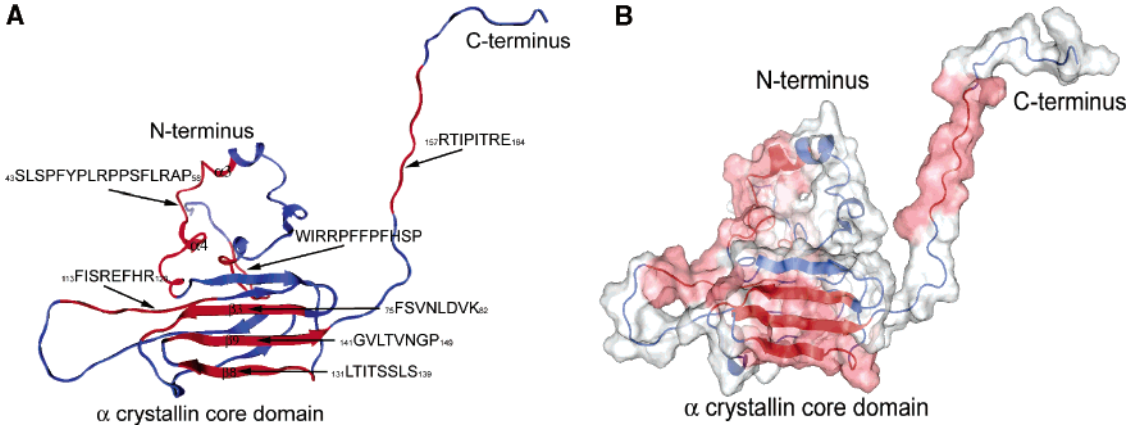

FIGURE 10: Three-dimensional map of the αB crystallin interactive domains. Interactive domains of human αB crystallin identified by the pin arrays are colored red, while noninteractive regions are colored blue. (A) Ribbon representation of the secondary and tertiary structure of human αB crystallin. The sequences $_{9}$WIRRPFFPFHSP$_{20}$, $_{113}$FISREFHR$_{120}$, and $_{157}$RTIPITRE$_{164}$ did not have secondary structure. The sequence $_{43}$SLSPFYLRPPSFLRAP$_{58}$, formed the α3−turn−α4 motif, while the sequences $_{75}$FSVNLDVK$_{82}$, $_{131}$LTITSSLS$_{138}$, and $_{141}$GVLTVNGP$_{148}$ formed β strand motifs β3, β8, and β9, respectively. (B) Solid models of the 3D structure of human αB crystallin. Surfaces of residues in the interactive domains $_{9}$WIRRPFFPFHSP$_{20}$, $_{43}$SLSPFYLRPPSFLRAP$_{58}$, $_{75}$FSVNLDVK$_{82}$, $_{113}$FISREFHR$_{120}$, $_{131}$LTITSSLS$_{138}$, $_{141}$GVLTVNGP$_{148}$, and $_{157}$RTIPITRE$_{164}$ that are solvent accessible are colored pink. The surfaces of residues in the noninteractive regions of αB crystallin are colored gray. Seventy-two percent of the collective accessible surface area of the N-terminal sequences $_{9}$WIRRPFFPFHSP$_{20}$ and $_{43}$SLSPFYLRPPSFLRAP$_{58}$ was hydrophobic; 67% of the collective accessible surface area of the α crystallin core domain sequences, $_{75}$FSVNLDVK$_{82}$ (β3), $_{131}$LTITSSLS$_{138}$ (β8), and $_{141}$GVLTVNGP$_{148}$ (β9), was hydrophobic. The loop region sequence $_{113}$FISREFHR$_{120}$ was 61% hydrophobic, and the C-terminal extension sequence $_{157}$RTIPITRE$_{164}$ was 59% hydrophobic.

hydrophobic peptides in the human αB crystallin protein pin array. On the basis of the hydrophobicity values provided by the manufacturer, the interactive peptides $_{9}$WIRRPFFPFHSP$_{20}$, $_{43}$SLSPFYLRPPSFLRAP$_{58}$, and $_{131}$LTITSSLS$_{138}$ were quite hydrophobic. Fourteen noninteractive peptides in the human αB crystallin pin array were more hydrophobic than the remaining interactive peptides, $_{75}$FSVNLDVK$_{82}$, $_{113}$FISREFHR$_{120}$, $_{141}$GVLTVNGP$_{148}$, and $_{157}$RTIPITRE$_{164}$ (*47*).

Far-UV CD analysis indicated that there was a <10% loss of secondary structure of β_H crystallin and γD crystallin when they were heated at 45 °C for 15 min. However, the magnitude of the absorption peaks in the near-UV CD spectra of β_H crystallin and γD crystallin decreased by ~20−25%, which indicated conformational changes in the tertiary structures of those proteins. In the absence of significant unfolding and loss of secondary structure of β_H crystallin and γD crystallin as determined by far-UV CD, the increased level of interaction between interactive αB crystallin peptides and preheated β_H crystallin and γD crystallin suggested that the interactive domains of αB crystallin detected conformational changes in tertiary structure that resulted from preheating β_H crystallin and γD crystallin. It appeared that the pin arrays are as sensitive as near-UV CD in detecting perturbations in the tertiary structure of unfolded proteins.

Two of the seven chaperone sequences were in the N-terminus and four in the conserved α crystallin core domain, and one was in the C-terminal extension containing the highly conserved I-X-I/V motif. The pin array results suggested that point mutations within the interactive domains can be expected to modify the chaperone activity of αB crystallin and point mutations outside the interactive domains can be expected to have little or no effect on chaperone activity. While systematic studies have not been reported for the sequence motifs identified using the pin arrays to date, literature results are consistent with the suggestion that the sequences identified by the pin arrays are important motifs for the chaperone-like activity of human αB crystallin (*63*, *70*−*75*). Mutagenesis of αB crystallin in which deletions of the C-terminal extension included arginine 157 resulted in diminished chaperone activity in vitro when compared to that of full-length αB crystallin (*76*). Arginine 157 is present in the $_{157}$RTIPITRE$_{164}$ chaperone sequence identified by the pin arrays. X-ray solution scattering on a truncation mutant of αB crystallin (αB crystallin 57−157) indicated that the α crystallin domain in the absence of the N- and C-terminal extensions formed dimers and had decreased chaperone-like activity in vitro as compared to full-length αB crystallin (*77*). When two consensus chaperone sequences ($_{73}$DRFSVNLDVKHFS$_{85}$ and $_{131}$LTITSSLSDGV$_{141}$) belonging to the α crystallin core domain were synthesized and tested for protection against thermal unfolding and aggregation of chaperone target proteins β_H crystallin, ADH, and CS in vitro, a substantial protective effect was observed. The chaperone assays confirmed that the sequences identified using the pin array were important for the chaperone activity of αB crystallin and were consistent with an earlier study in which hydrophobic probes and chaperone assays identified the αB crystallin sequence $_{73}$DRFSVNLDVK$_{82}$ as an interactive sequence for chaperone activity (*78*). Selected point or combination mutations in the interactive sequences of αB crystallin can be expected to improve or diminish chaperone activity. A higher concentration of both peptides was required to protect against the aggregation of β_H crystallin and ADH than to protect against the aggregation of CS. Circular dichroism analysis indicated that β_H crystallin was partially unfolded and both ADH and CS were almost completely unfolded at 50 °C. Taken together, the chaperone assay and circular dichroism data suggested that the peptides were more efficient in protecting against the aggregation of a completely unfolded protein and less efficient in protecting against the aggregation of partially unfolded or nativelike proteins.

The interactive sequences identified using the pin arrays were mapped onto a 3D model of αB crystallin to analyze the structural topography of the chaperone interface (*47*). In the absence of an X-ray crystal or NMR structure, it was

observed that superposition of the computed αB crystallin homology model with the crystal structure of Mj sHSP16.5 and wheat sHSP16.9 was remarkable with a Cα root-mean-square deviation of 2.06 Å for the α crystallin core domain (*39*, *45*). Secondary structure was assigned to the interactive sequences identified by the pin arrays on the basis of electron paramagnetic resonance data (EPR) and a multiple-sequence alignment of human αB crystallin with the crystal structures of wheat sHSP16.9 and Mj sHSP16.5 (*39*, *45*, *58*, *62*). The N-terminal chaperone sequence, $_{9}$WIRRPFFPFHSP$_{20}$, was unstructured and formed a surface that was 70% hydrophobic, while the sequence $_{43}$SLSPFYLRPPSF$_{54}$ formed a helix−turn−helix motif with an external surface that was 72% hydrophobic and favorable for binding exposed hydrophobic patches of unfolding proteins. Three of the four sequences in the α crystallin core domain [$_{75}$FSVNLDVK$_{82}$ (β3), $_{131}$LTITSSLS$_{138}$ (β8), and $_{141}$GVLTVNGP$_{148}$ (β9)] were β strands and formed a surface that was 67% hydrophobic. The C-terminal chaperone sequence $_{157}$RTIPITRE$_{164}$ containing the highly conserved I-X-I/V motif was unstructured and formed a surface that was 59% hydrophobic. The chaperone sequences $_{43}$SLSPFYLRPPSF$_{54}$, $_{75}$FSVNLDVK$_{82}$, $_{131}$LTITSSLS$_{138}$, $_{141}$GVLTVNGP$_{148}$, and $_{157}$RTIPITRE$_{164}$ identified in this report overlapped significantly with sequences identified previously as subunit−subunit interaction sites in αB crystallin using protein pin arrays (Figure 9, shaded residues) (*47*). The sequence $_{43}$SLSPFYLRPPSF$_{54}$ identified by the pin arrays is a subset of the sequence $_{42}$TSLSPFYLRPPSFLRA$_{57}$, previously reported as an interactive region in αB crystallin that interacts with human αA crystallin (*50*, *51*). Both synthesized peptides, $_{73}$DRFSVNLDVKHFS$_{85}$ and $_{131}$LTITSSLSDGV$_{141}$, that protected β_{H} crystallin, ADH, and CS from aggregation were previously identified as interactive sequences for subunit−subunit interactions in αB crystallin (*47*). The results suggested that interactive sequences in αB crystallin may have dual roles in subunit assembly and chaperone function, which is consistent with previous mutagenesis data in which loss of chaperone function was accompanied by decreased assembly size (*49*, *79*). The identification of common sequences for subunit−subunit interactions and chaperone activity in αB crystallin by the pin arrays suggests that dissociation of αB crystallin complexes may be required for the exposure of chaperone sequences that can bind unfolding chaperone target proteins. This hypothesis is consistent with previous studies of the role of oligomeric equilibrium in regulating the chaperone activity of HSP27 and αB crystallin (*80*, *81*). Shashidharamurthy et al. (*80*) reported that dissociation of the HSP27 oligomer was required for interactions with destabilized T4 lysozyme mutants. Srinivas et al. (*81*) reported that arginine hydrochloride enhanced the chaperone activity of αB crystallin by accelerating its subunit−subunit dynamics.

The lack of interactive sequences similar to the αB crystallin N-terminal and C-terminal chaperone sequences, $_{9}$WIRRPFFPFHSP$_{20}$, $_{43}$SLSPFYLRPPSFLRAP$_{58}$, and $_{157}$RTIPITRE$_{164}$, in sHSPs of *C. elegans* (sHSP12.2, sHSP12.3, and sHSP12.6, respectively) could account for the absence of chaperone-like activity of *C. elegans* sHSPs in vitro (*82*). The interface formed by the α crystallin core domain peptides $_{75}$FSVNLDVK$_{82}$ (β3), $_{131}$LTITSSLS$_{138}$ (β8), and $_{141}$GVLTVNGP$_{148}$ (β9) that interacted with all four chaperone target proteins and collectively formed an external surface that was 67% hydrophobic was previously identified as the interface for the assembly of human αB crystallin subunits using pin arrays (*47*). The interface provides residues for both hydrophobic and hydrophilic interactions with native proteins (αA and αB crystallin) as well as with unfolding chaperone target proteins (β_{H} crystallin and γD crystallin). The structure of the α crystallin core domain is highly conserved in the small heat shock protein family, and sequences homologous to the αB crystallin chaperone sequences $_{75}$FSVNLDVK$_{82}$, $_{113}$FISREFHR$_{120}$, $_{131}$LTITSSLS$_{138}$, and $_{141}$GVLTVNGP$_{148}$ in other small heat shock proteins are expected to be involved in the chaperone function of other sHSPs. In summary, pin array assays, in vitro chaperone assays, and circular dichroism spectroscopy of target proteins identified the sequences in full-length αB crystallin that were responsible for interactions with a broad range of target proteins, including proteins that are almost completely unfolded (ADH and CS) and proteins that are partially unfolded (β_{H} crystallin and γD crystallin). Protein pin arrays were effective in identifying protein−protein interactive domains in human αB crystallin that were important in oligomeric assembly and in interactions with unfolding chaperone target proteins. Further investigation of the specific sequences and 3D structures of the interactive domains in physiologically relevant small heat shock proteins, including human sHSP27 and *Mycobacterium tuberculosis* sHSP16.3, will provide new information about the function of sHSPs and molecular chaperones in disease. Our results suggest that the collective response of sHSPs to protein unfolding involves several interactive domains and that sHSPs are exquisitely sensitive to protein unfolding. These results could account for the selectivity and sensitivity of small heat shock proteins and their adaptation to the needs of specific cells and their response to stress.

ACKNOWLEDGMENT

We thank Christophe Verlinde, Elinor Adman, Andrew Farr, and James Dooley for technical support. We thank Tracy Cranick for help with preparation of the manuscript.

REFERENCES

1. Ingolia, T. D., and Craig, E. A. (1982) Four small *Drosophila* heat shock proteins are related to each other and to mammalian α-crystallin, *Proc. Natl. Acad. Sci. U.S.A. 79*, 2360−4.
2. Klemenz, R., Frohli, E., Steiger, R. H., Schafer, R., and Aoyama, A. (1991) αB-Crystallin is a small heat shock protein, *Proc. Natl. Acad. Sci. U.S.A. 88*, 3652−6.
3. Merck, K. B., Groenen, P. J., Voorter, C. E., de Haard-Hoekman, W. A., Horwitz, J., Bloemendal, H., and de Jong, W. W. (1993) Structural and functional similarities of bovine α-crystallin and mouse small heat-shock protein. A family of chaperones, *J. Biol. Chem. 268*, 1046−52.
4. de Jong, W. W., Leunissen, J. A., and Voorter, C. E. (1993) Evolution of the α-crystallin/small heat-shock protein family, *Mol. Biol. Evol. 10*, 103−26.
5. Groenen, P. J., Merck, K. B., de Jong, W. W., and Bloemendal, H. (1994) Structure and modifications of the junior chaperone α-crystallin. From lens transparency to molecular pathology, *Eur. J. Biochem. 225*, 1−19.
6. de Jong, W. W., Caspers, G. J., and Leunissen, J. A. (1998) Genealogy of the α-crystallin: Small heat-shock protein superfamily, *Int. J. Biol. Macromol. 22*, 151−62.
7. Bloemendal, H., de Jong, W., Jaenicke, R., Lubsen, N. H., Slingsby, C., and Tardieu, A. (2004) Ageing and vision: Structure, stability and function of lens crystallins, *Prog. Biophys. Mol. Biol. 86*, 407−85.

8. Iwaki, T., Kume-Iwaki, A., Liem, R. K., and Goldman, J. E. (1989) αB-Crystallin is expressed in non-lenticular tissues and accumulates in Alexander's disease brain, *Cell 57*, 71−8.
9. Iwaki, T., Wisniewski, T., Iwaki, A., Corbin, E., Tomokane, N., Tateishi, J., and Goldman, J. E. (1992) Accumulation of αB-crystallin in central nervous system glia and neurons in pathologic conditions, *Am. J. Pathol. 140*, 345−56.
10. Kato, S., Hirano, A., Umahara, T., Llena, J. F., Herz, F., and Ohama, E. (1992) Ultrastructural and immunohistochemical studies on ballooned cortical neurons in Creutzfeldt-Jakob disease: Expression of αB-crystallin, ubiquitin and stress-response protein 27, *Acta Neuropathol. 84*, 443−8.
11. Shinohara, H., Inaguma, Y., Goto, S., Inagaki, T., and Kato, K. (1993) αB crystallin and HSP28 are enhanced in the cerebral cortex of patients with Alzheimer's disease, *J. Neurol. Sci. 119*, 203−8.
12. Goebel, H. H., and Bornemann, A. (1993) Desmin pathology in neuromuscular diseases, *Virchows Arch. B 64*, 127−35.
13. van Noort, J. M., van Sechel, A. C., Bajramovic, J. J., el Ouagmiri, M., Polman, C. H., Lassmann, H., and Ravid, R. (1995) The small heat-shock protein αB-crystallin as candidate autoantigen in multiple sclerosis, *Nature 375*, 798−801.
14. Jackson, M., Gentleman, S., Lennox, G., Ward, L., Gray, T., Randall, K., Morrell, K., and Lowe, J. (1995) The cortical neuritic pathology of Huntington's disease, *Neuropathol. Appl. Neurobiol. 21*, 18−26.
15. Lobrinus, J. A., Janzer, R. C., Kuntzer, T., Matthieu, J. M., Pfend, G., Goy, J. J., and Bogousslavsky, J. (1998) Familial cardiomyopathy and distal myopathy with abnormal desmin accumulation and migration, *Neuromuscular Disord. 8*, 77−86.
16. Renkawek, K., Stege, G. J., and Bosman, G. J. (1999) Dementia, gliosis and expression of the small heat shock proteins hsp27 and αB-crystallin in Parkinson's disease, *NeuroReport 10*, 2273−6.
17. van Rijk, A. F., and Bloemendal, H. (2000) αB-Crystallin in neuropathology, *Ophthalmologica 214*, 7−12.
18. Yeboah, F. A., and White, D. (2001) αB-Crystallin expression in celiac disease: A preliminary study, *Croat. Med. J. 42*, 523−6.
19. Garland, D., Russell, P., and Zigler, J. S., Jr. (1988) The oxidative modification of lens proteins, *Basic Life Sci. 49*, 347−52.
20. Harding, J. J. (1991) Post-translational modification of lens proteins in cataract, *Lens Eye Toxic. Res. 8*, 245−50.
21. Miesbauer, L. R., Zhou, X., Yang, Z., Sun, Y., Smith, D. L., and Smith, J. B. (1994) Post-translational modifications of water-soluble human lens crystallins from young adults, *J. Biol. Chem. 269*, 12494−502.
22. Goode, D., and Crabbe, M. J. (1995) Modelling molecular stability in γB crystallin, *Comput. Chem. 19*, 65−74.
23. Lund, A. L., Smith, J. B., and Smith, D. L. (1996) Modifications of the water-insoluble human lens α-crystallins, *Exp. Eye Res. 63*, 661−72.
24. Hanson, S. R., Smith, D. L., and Smith, J. B. (1998) Deamidation and disulfide bonding in human lens γ-crystallins, *Exp. Eye Res. 67*, 301−12.
25. Yan, H., and Hui, Y. (2000) [The recent progress on the role of α-crystallin as a molecular chaperone in cataractogenesis], *Yan Ke Xue Bao 16*, 91−6.
26. Feng, J., Smith, D. L., and Smith, J. B. (2000) Human lens β-crystallin solubility, *J. Biol. Chem. 275*, 11585−90.
27. Garner, B., Shaw, D. C., Lindner, R. A., Carver, J. A., and Truscott, R. J. (2000) Non-oxidative modification of lens crystallins by kynurenine: A novel post-translational protein modification with possible relevance to ageing and cataract, *Biochim. Biophys. Acta 1476*, 265−78.
28. Lapko, V. N., Smith, D. L., and Smith, J. B. (2001) In vivo carbamylation and acetylation of water-soluble human lens αB-crystallin lysine 92, *Protein Sci. 10*, 1130−6.
29. Kim, Y. H., Kapfer, D. M., Boekhorst, J., Lubsen, N. H., Bachinger, H. P., Shearer, T. R., David, L. L., Feix, J. B., and Lampi, K. J. (2002) Deamidation, but not truncation, decreases the urea stability of a lens structural protein, βB1-crystallin, *Biochemistry 41*, 14076−84.
30. Ueda, Y., Duncan, M. K., and David, L. L. (2002) Lens proteomics: The accumulation of crystallin modifications in the mouse lens with age, *Invest. Ophthalmol. Visual Sci. 43*, 205−15.
31. Fu, L., and Liang, J. J. (2003) Alteration of protein−protein interactions of congenital cataract crystallin mutants, *Invest. Ophthalmol. Visual Sci. 44*, 1155−9.
32. Srivastava, O. P., and Srivastava, K. (2003) Existence of deamidated αB-crystallin fragments in normal and cataractous human lenses, *Mol. Vision 9*, 110−8.
33. del Valle, L. J., Escribano, C., Perez, J. J., and Garriga, P. (2002) Calcium-induced decrease of the thermal stability and chaperone activity of α-crystallin, *Biochim. Biophys. Acta 1601*, 100−9.
34. Slingsby, C., and Clout, N. J. (1999) Structure of the crystallins, *Eye 13* (Part 3b), 395−402.
35. Hook, D. W., and Harding, J. J. (1998) Protection of enzymes by α-crystallin acting as a molecular chaperone, *Int. J. Biol. Macromol. 22*, 295−306.
36. Takemoto, L., and Boyle, D. (1998) The possible role of α-crystallins in human senile cataractogenesis, *Int. J. Biol. Macromol. 22*, 331−7.
37. Fu, L., and Liang, J. J. (2002) Detection of protein−protein interactions among lens crystallins in a mammalian two-hybrid system assay, *J. Biol. Chem. 277*, 4255−60.
38. Nicholl, I. D., and Quinlan, R. A. (1994) Chaperone activity of α-crystallins modulates intermediate filament assembly, *EMBO J. 13*, 945−53.
39. Kim, K. K., Kim, R., and Kim, S. H. (1998) Crystal structure of a small heat-shock protein, *Nature 394*, 595−9.
40. Basak, A., Bateman, O., Slingsby, C., Pande, A., Asherie, N., Ogun, O., Benedek, G. B., and Pande, J. (2003) High-resolution X-ray crystal structures of human γD crystallin (1.25 Å) and the R58H mutant (1.15 Å) associated with aculeiform cataract, *J. Mol. Biol. 328*, 1137−47.
41. Purkiss, A. G., Bateman, O. A., Goodfellow, J. M., Lubsen, N. H., and Slingsby, C. (2002) The X-ray crystal structure of human γS-crystallin C-terminal domain, *J. Biol. Chem. 277*, 4199−205.
42. Sergeev, Y. V., David, L. L., Chen, H. C., Hope, J. N., and Hejtmancik, J. F. (1998) Local microdomain structure in the terminal extensions of βA3- and βB2-crystallins, *Mol. Vision 4*, 9.
43. Hejtmancik, J. F., Wingfield, P. T., Chambers, C., Russell, P., Chen, H. C., Sergeev, Y. V., and Hope, J. N. (1997) Association properties of βB2- and βA3-crystallin: Ability to form dimers, *Protein Eng. 10*, 1347−52.
44. Norledge, B. V., Trinkl, S., Jaenicke, R., and Slingsby, C. (1997) The X-ray structure of a mutant eye lens βB2-crystallin with truncated sequence extensions, *Protein Sci. 6*, 1612−20.
45. van Montfort, R. L., Basha, E., Friedrich, K. L., Slingsby, C., and Vierling, E. (2001) Crystal structure and assembly of a eukaryotic small heat shock protein, *Nat. Struct. Biol. 8*, 1025−30.
46. Carver, J. A., and Lindner, R. A. (1998) NMR spectroscopy of α-crystallin. Insights into the structure, interactions and chaperone action of small heat-shock proteins, *Int. J. Biol. Macromol. 22*, 197−209.
47. Ghosh, J. G., and Clark, J. I. (2005) Insights into the domains required for dimerization and assembly of human αB crystallin, *Protein Sci. 14*, 684−95.
48. Kokke, B. P., Boelens, W. C., and de Jong, W. W. (2001) The lack of chaperonelike activity of *Caenorhabditis elegans* Hsp12.2 cannot be restored by domain swapping with human αB-crystallin, *Cell Stress Chaperones 6*, 360−7.
49. Saha, S., and Das, K. P. (2004) Relationship between chaperone activity and oligomeric size of recombinant human αA- and αB-crystallin: A tryptic digestion study, *Proteins 57*, 610−7.
50. Sreelakshmi, Y., Santhoshkumar, P., Bhattacharyya, J., and Sharma, K. K. (2004) αA-Crystallin Interacting Regions in the Small Heat Shock Protein, αB-Crystallin, *Biochemistry 43*, 15785−95.
51. Lentze, N., and Narberhaus, F. (2004) Detection of oligomerisation and substrate recognition sites of small heat shock proteins by peptide arrays, *Biochem. Biophys. Res. Commun. 325*, 401−7.
52. Sharma, K. K., Kumar, R. S., Kumar, G. S., and Quinn, P. T. (2000) Synthesis and characterization of a peptide identified as a functional element in αA-crystallin, *J. Biol. Chem. 275*, 3767−71.
53. Geysen, H. M. (1990) Molecular technology: Peptide epitope mapping and the pin technology, *Southeast Asian J. Trop. Med. Public Health 21*, 523−33.
54. Chin, J., Fell, B., Shapiro, M. J., Tomesch, J., Wareing, J. R., and Bray, A. M. (1997) Magic Angle Spinning NMR for Reaction Monitoring and Structure Determination of Molecules Attached to Multipin Crowns, *J. Org. Chem. 62*, 538−9.
55. Fechteler, T., Dengler, U., and Schomburg, D. (1995) Prediction of protein three-dimensional structures in insertion and deletion regions: A procedure for searching data bases of representative

protein fragments using geometric scoring criteria, *J. Mol. Biol. 253*, 114−31.
56. Jeanmougin, F., Thompson, J. D., Gouy, M., Higgins, D. G., and Gibson, T. J. (1998) Multiple sequence alignment with Clustal X, *Trends Biochem. Sci. 23*, 403−5.
57. Aiyar, A. (2000) The use of CLUSTAL W and CLUSTAL X for multiple sequence alignment, *Methods Mol. Biol. 132*, 221−41.
58. Koteiche, H. A., and McHaourab, H. S. (1999) Folding pattern of the α-crystallin domain in αA-crystallin determined by site-directed spin labeling, *J. Mol. Biol. 294*, 561−77.
59. Morris, A. L., MacArthur, M. W., Hutchinson, E. G., and Thornton, J. M. (1992) Stereochemical quality of protein structure coordinates, *Proteins 12*, 345−64.
60. Guruprasad, K., and Kumari, K. (2003) Three-dimensional models corresponding to the C-terminal domain of human αA- and αB-crystallins based on the crystal structure of the small heat-shock protein HSP16.9 from wheat, *Int. J. Biol. Macromol. 33*, 107−12.
61. Berengian, A. R., Bova, M. P., and McHaourab, H. S. (1997) Structure and function of the conserved domain in αA-crystallin. Site-directed spin labeling identifies a *β*-strand located near a subunit interface, *Biochemistry 36*, 9951−7.
62. Koteiche, H. A., Berengian, A. R., and McHaourab, H. S. (1998) Identification of protein folding patterns using site-directed spin labeling. Structural characterization of a *β*-sheet and putative substrate binding regions in the conserved domain of αA-crystallin, *Biochemistry 37*, 12681−8.
63. Muchowski, P. J., Wu, G. J., Liang, J. J., Adman, E. T., and Clark, J. I. (1999) Site-directed mutations within the core "α-crystallin" domain of the small heat-shock protein, human αB-crystallin, decrease molecular chaperone functions, *J. Mol. Biol. 289*, 397−411.
64. Sharma, K. K., Kaur, H., and Kester, K. (1997) Functional elements in molecular chaperone α-crystallin: Identification of binding sites in αB-crystallin, *Biochem. Biophys. Res. Commun. 239*, 217−22.
65. Sharma, K. K., Kumar, G. S., Murphy, A. S., and Kester, K. (1998) Identification of 1,1′-bi(4-anilino)naphthalene-5,5′-disulfonic acid binding sequences in α-crystallin, *J. Biol. Chem. 273*, 15474−8.
66. Sharma, K. K., Kaur, H., Kumar, G. S., and Kester, K. (1998) Interaction of 1,1′-bi(4-anilino)naphthalene-5,5′-disulfonic acid with α-crystallin, *J. Biol. Chem. 273*, 8965−70.
67. Singh, R., and Rao, C. M. (2002) Chaperone-like activity and surface hydrophobicity of 70S ribosome, *FEBS Lett. 527*, 234−8.
68. Srinivas, V., Datta, S. A., Ramakrishna, T., and Rao, C. M. (2001) Studies on the α-crystallin target protein binding sites: Sequential binding with two target proteins, *Mol. Vision 7*, 114−9.
69. Rajaraman, K., Raman, B., Ramakrishna, T., and Rao, C. M. (2001) Interaction of human recombinant αA- and αB-crystallins with early and late unfolding intermediates of citrate synthase on its thermal denaturation, *FEBS Lett. 497*, 118−23.
70. Gupta, R., and Srivastava, O. P. (2004) Effect of deamidation of asparagine 146 on functional and structural properties of human lens αB-crystallin, *Invest. Ophthalmol. Visual Sci. 45*, 206−14.
71. Liao, J. H., Lee, J. S., and Chiou, S. H. (2002) C-Terminal lysine truncation increases thermostability and enhances chaperone-like function of porcine αB-crystallin, *Biochem. Biophys. Res. Commun. 297*, 309−16.
72. Kumar, L. V., Ramakrishna, T., and Rao, C. M. (1999) Structural and functional consequences of the mutation of a conserved arginine residue in αA and αB crystallins, *J. Biol. Chem. 274*, 24137−41.
73. Horwitz, J., Bova, M., Huang, Q. L., Ding, L., Yaron, O., and Lowman, S. (1998) Mutation of αB-crystallin: Effects on chaperone-like activity, *Int. J. Biol. Macromol. 22*, 263−9.
74. Plater, M. L., Goode, D., and Crabbe, M. J. (1996) Effects of site-directed mutations on the chaperone-like activity of αB-crystallin, *J. Biol. Chem. 271*, 28558−66.
75. Derham, B. K., van Boekel, M. A., Muchowski, P. J., Clark, J. I., Horwitz, J., Hepburne-Scott, H. W., de Jong, W. W., Crabbe, M. J., and Harding, J. J. (2001) Chaperone function of mutant versions of αA- and αB-crystallin prepared to pinpoint chaperone binding sites, *Eur. J. Biochem. 268*, 713−21.
76. Thampi, P., and Abraham, E. C. (2003) Influence of the C-terminal residues on oligomerization of αA-crystallin, *Biochemistry 42*, 11857−63.
77. Feil, I. K., Malfois, M., Hendle, J., van Der Zandt, H., and Svergun, D. I. (2001) A novel quaternary structure of the dimeric α-crystallin domain with chaperone-like activity, *J. Biol. Chem. 276*, 12024−9.
78. Sharma, S., Sathyanarayana, B. K., Bird, J. G., Hoskins, J. R., Lee, B., and Wickner, S. (2004) Plasmid P1 RepA is homologous to the F plasmid RepE class of initiators, *J. Biol. Chem. 279*, 6027−34.
79. Feil, C., and Augustin, H. G. (1998) Endothelial cells differentially express functional CXC-chemokine receptor-4 (CXCR-4/fusin) under the control of autocrine activity and exogenous cytokines, *Biochem. Biophys. Res. Commun. 247*, 38−45.
80. Shashidharamurthy, R., Koteiche, H. A., Dong, J., and McHaourab, H. S. (2005) Mechanism of chaperone function in small heat shock proteins: Dissociation of the HSP27 oligomer is required for recognition and binding of destabilized T4 lysozyme, *J. Biol. Chem. 280*, 5281−9.
81. Srinivas, V., Raman, B., Rao, K. S., Ramakrishna, T., and Rao, C. M. (2005) Arginine hydrochloride enhances the dynamics of subunit assembly and the chaperone-like activity of α-crystallin, *Mol. Vision 11*, 249−55.
82. Kokke, B. P., Leroux, M. R., Candido, E. P., Boelens, W. C., and de Jong, W. W. (1998) *Caenorhabditis elegans* small heat-shock proteins Hsp12.2 and Hsp12.3 form tetramers and have no chaperone-like activity, *FEBS Lett. 433*, 228−32.
83. Bloemendal, M., Toumadje, A., and Johnson, W. C., Jr. (1999) Bovine lens crystallins do contain helical structure: A circular dichroism study, *Biochim. Biophys. Acta 1432*, 234−8.
84. Lampi, K. J., Oxford, J. T., Bachinger, H. P., Shearer, T. R., David, L. L., and Kapfer, D. M. (2001) Deamidation of human *β* B1 alters the elongated structure of the dimer, *Exp. Eye Res. 72*, 279−88.

BI0503910